

1 **Assessment of tobacco and *N. benthamiana* as biofactories of irregular**
2 **monoterpenes for sustainable crop protection.**

3
4

5 Rubén Mateos-Fernández¹, Sandra Vacas², Ismael Navarro-Fuertes³, Vicente Navarro-Llopis², Diego
6 Orzáez^{1†} and Silvia Gianoglio¹

7
8
9

¹ Instituto de Biología Molecular y Celular de Plantas, CSIC-Universitat Politècnica de València, 46022, Valencia, Spain

10 ² Centro de Ecología Química Agrícola, Instituto Agroforestal del Mediterráneo, Universitat Politècnica de València, 46022 Valencia,
11 Spain

12 ³ Department of Organic Chemistry, Universitat de València, 46010 Valencia, Spain

13
14

† To whom correspondence should be addressed

15
16
17
18

19 Rubén Mateos-Fernández: rumafer@doctor.upv.es
20 Sandra Vacas: sanvagon@ceqa.upv.es
21 Ismael Navarro-Fuertes: ismael.navarro-fuertes@uv.es
22 Vicente Navarro-Llopis: vinallo@ceqa.upv.es
23 Diego Orzáez: dorzaez@ibmcp.upv.es
24 Silvia Gianoglio: sgianog@ibmcp.upv.es

25
26
27
28
29
30
31

32 **ABSTRACT**

33 Irregular monoterpenes are important precursors of different compounds employed in pest control such as
34 insecticides and insect sex pheromones. Metabolically engineered plants are appealing as biofactories of
35 such compounds, but specially as potential live biodispensers of related bioactive volatiles, which could be
36 continuously emitted to the environment from different plant tissues. Here we assess the use of cultivated
37 tobacco and *Nicotiana benthamiana* as biofactories for the irregular monoterpenes chrysanthemol and
38 lavandulol. We evaluate the impact of high levels of constitutive metabolite production on the plant
39 physiology and biomass, and their biosynthetic dynamics for different plant tissues and developmental
40 stages. As an example of an active pheromone compound, we super-transformed the best lavandulol-
41 producing tobacco line with an acetyl transferase gene to obtain a tobacco lavandulyl acetate biodispenser
42 emitting up to 0.63 mg of lavandulyl acetate per plant every day. We estimate that with these volatile
43 emission levels, between 200 and 500 plants per hectare would be sufficient to ensure a daily emission of
44 pheromones comparable to commercial lures. This is an important step towards plant-based sustainable
45 solutions for pest control, and it lays the ground for further developing biofactories for other irregular
46 monoterpenoid pheromones, whose biosynthetic genes are yet unknown.

47

48

49 **KEYWORDS**

50 Biofactories; irregular monoterpenes; mealybugs; *Nicotiana benthamiana*; pheromones; tobacco.

51

52 Introduction

53 Sustainability in agri-food systems, as in any other sector of the economy, is achieved by balancing the long-
54 term – and sometimes competing – interests of environmental protection, economic profitability and social
55 equity. The protection of crops and stored goods from damage induced by insect pests is an indispensable
56 aspect of increasing agricultural yields and reducing food waste, and the way in which pest control is achieved
57 is fundamental for sustainability. Insect pheromones are sustainable alternatives to traditional pesticides
58 because they are effective, safe, and pose very limited risks of insurgence of genetic resistance, with virtually
59 inexistent effects on non-target populations (Rizvi *et al.*, 2021). Pheromones are volatile organic compounds
60 (VOCs) produced by insects that function at very low concentrations as semiochemicals modulating the
61 behavior of conspecifics. The most interesting for pest control are sex pheromones, usually produced by
62 females, and aggregation pheromones, mainly produced by males to attract both males and females. Both
63 types of pheromones can be used as lures to construct traps to attract and affect individuals, or to monitor
64 population levels. Sex pheromones are also employed in mating disruption strategies, where the release of
65 the pheromone to the environment masks the signal produced by females, preventing or delaying mating
66 (Miller & Gut, 2015). Despite their advantages, the chemical synthesis of pheromone compounds and the
67 formulation of traps can be complex and costly, making them affordable for expensive end products (like
68 high-value orchard productions), but far less accessible for row crops (Bento *et al.*, 2016; Ioriatti & Lucchi,
69 2016; Petkevicius *et al.*, 2020). Thus, research has focused on developing pheromone biofactories through
70 the engineering of biological hosts like yeasts and plants (Mateos Fernández *et al.*, 2022). Bioproduction of
71 pheromones has, in principle, several advantages over chemical synthesis: renewable feedstocks benefit the
72 production pipeline and generate fewer polluting by-products; production costs are reduced; finally,
73 chemical synthesis produces racemic mixtures, while enzymes ensure stereoselectivity, which is crucial for
74 pheromone activity (Mateos Fernández *et al.*, 2022). Biofactories can be used either to synthesize active
75 pheromone compounds (Ding *et al.*, 2014; Holkenbrink *et al.*, 2020; Mateos-Fernández *et al.*, 2021), or to
76 produce precursors to be extracted and modified chemically, resulting in hemisynthetic preparations that
77 still enhance sustainability (Nešňorová *et al.*, 2004; Xia *et al.*, 2020; Wang *et al.*, 2022). While yeasts can
78 provide greater yields and ease of extraction, plants may be used as pheromone biofactories following two
79 different strategies: one is to synthesize molecules (active compounds or precursors) to be extracted; the
80 second is to engineer plants to be live pheromone emitters (Bruce *et al.*, 2015). The appropriate plant host
81 for each strategy depends on plant biomass, on specialized metabolisms supporting the production of target
82 compounds and, for bioemitters, on the ability to volatilize them.

83 The bulk of pheromone bioproduction has focused on Lepidopteran sex pheromones, because of the
84 enormous economic relevance of these pests and because these molecules have relatively simple structures
85 and their biosynthetic pathways are known (Löfstedt *et al.*, 2016). Still, an immense potential exists to
86 produce a wide variety of pheromones for different targets. Mealybugs (Pseudococcidae) are a family of
87 insects which constitute a relevant threat to crops in sub-tropical and Mediterranean climates. Their mating
88 behavior strongly depends on sex pheromones: these typically contain various monoterpene-derived esters
89 and many species synthesize irregular monoterpenes, which are unusual in nature, resulting from the non-
90 head-to-tail coupling of two DMAPP units instead of the regular (head-to-tail) condensation of an IPP and a
91 DMAPP unit (Kobayashi & Kuzuyama, 2019). Zou & Millar (2015) provide an extensive review of mealybug
92 sex pheromones and their chemistry. Unfortunately, their biosynthesis remains unclear and insect genes
93 responsible for their production are yet to be identified (Tabata, 2022; Juteršek *et al.*, 2023). In the absence
94 of known mealybug biosynthetic genes, alternative approaches to the bioproduction of their sex pheromones
95 rely on other organisms producing analogous compounds. This is the case of plants producing lavandulyl
96 pyrophosphate (LPP) and chrysanthemyl pyrophosphate (CPP), irregular branched and cyclic
97 monoterpenoids, respectively (Figure 1A). LPP and its derivatives lavandulol and lavandulyl acetate are
98 produced by various lavender species (Lamiaceae) and by some Apiaceae and are important fragrances, while

99 CPP and the alcohol chrysanthemol are produced by members of the Anthemidae tribe within the Asteraceae
100 family (Minteguiaga *et al.*, 2023). LPP and CPP are the precursors of a variety of bioactive compounds
101 important for pest management. Both LPP and CPP are valuable as the monoterpene moieties of the sex
102 pheromone compounds of various mealybug species (such as *Planococcus ficus* Signoret, *Dysmicoccus grassii*
103 Leonardi and *Phenacoccus madeirensis* Green, among others) and can be easily esterified to give an active
104 product (Zou & Millar, 2015). In particular, lavandulyl acetate is an active pheromone compound for the
105 mealybug *D. grassii* (De Alfonso *et al.*, 2012), and a component of the aggregation pheromone of the Western
106 flower thrips *Frankliniella occidentalis* Pergrande (Hamilton *et al.*, 2005). Finally, lavandulyl acetate has also
107 been identified as a mosquito larvicide with low toxicity towards non-target organisms (Govindarajan &
108 Benelli, 2016), and CPP is a precursor for the biosynthesis of pyrethrins, a class of important natural
109 insecticides (Xu *et al.*, 2018).

110 Monoterpenoids are highly accumulated by common aromatic plants, which store essential oil compounds
111 in glandular trichomes. However, these plants are not ideal bioproduction platforms for heterologous
112 compounds, since they are not easy to transform genetically, and their biomass and growth rate are lower
113 than other wide-leaf species, such as tobacco (*Nicotiana tabacum* L.) and *Nicotiana benthamiana* Domin.
114 Tobacco represents a versatile chassis for genetic manipulation with high biomass production, and *N.*
115 *benthamiana* allows efficient testing of multiple gene combinations through agroinfiltration (Molina-Hidalgo
116 *et al.*, 2021). Thus, we used the LPP synthase gene from *Lavandula x intermedia* Emeric ex Loisel. (*LiLPPS*;
117 Demissie *et al.*, 2013) and the CPP synthase gene from *Tanacetum cinerariifolium* (Trevir.) Sch.Bip. (*TcCPPS*;
118 Yang *et al.*, 2014) to transform tobacco and *N. benthamiana*, aiming at assessing the potential of these
119 species as producers and emitters of irregular monoterpenoids. We also transformed *LiLPPS*-expressing
120 tobacco plants with the AAT4 acetyltransferase from *L. intermedia* (Sarker & Mahmoud, 2015), successfully
121 esterifying lavandulol to lavandulyl acetate.

122 Materials and methods

123 DNA assembly and cloning

124 All DNA parts used for plant transformation were domesticated and assembled using the GoldenBraid
125 standard as described by Sarrion-Perdigones *et al.* (2011). All constructs were verified by Sanger sequencing
126 and/or restriction analysis. All GB constructs designed and employed in this study are available at
127 www.gbcloning.upv.es under their corresponding IDs, which are listed in Supplementary Table S1. All
128 constructs were cloned using the *Escherichia coli* TOP 10 strain. The final expression vectors were
129 transformed into electrocompetent *Agrobacterium tumefaciens* GV3101 or LBA4404 for transient or stable
130 transformations, respectively.

131 Transient expression assays in *Nicotiana benthamiana*

132 Transient expression assays to validate gene activity were carried out through infiltration of *N. benthamiana*
133 leaves mediated by *Agrobacterium tumefaciens*. Pre-cultures were grown from glycerol stocks for two days
134 at 28°C at 250 rpm with the appropriate antibiotics until saturation, then refreshed and grown overnight in
135 the same conditions. Cells were pelleted and resuspended in an agroinfiltration buffer containing 10 mM 2-
136 (N-morpholino) ethanesulfonic acid (MES), pH 5.7, 10 mM MgCl₂, and 200 μM acetosyringone, then
137 incubated for 2h at RT under slow shaking. The OD₆₀₀ of each culture was adjusted to reach a value of 0.05-
138 0.06 in the final culture mixtures. Each mixture had a final OD₆₀₀ value of 0.2. Equal volumes of each culture
139 were mixed, including the silencing suppressor P19 for co-infiltration to reduce post-transcriptional gene
140 silencing (Garabagi *et al.*, 2012). The relative abundance of each *A. tumefaciens* culture was kept constant in
141 all infiltration mixtures by adding an *A. tumefaciens* culture carrying an empty vector when needed.
142 Agroinfiltration was carried out with a 1 mL needle-free syringe, through the abaxial surface of the three
143 youngest fully expanded leaves of 4-5 weeks old *N. benthamiana* plants, grown at 24°C (light)/20°C (darkness)
144 with a 16:8 h light:darkness photoperiod. Samples were collected 5 days post-agroinfiltration using a Ø 1.5-
145 2 cm corkborer and snap frozen in liquid nitrogen.

146 Generation and selection of stable transformants

147 Stable transgenic plants were generated following the transformation protocol described by Kallam *et al.*
148 (2023). The same procedure was used for tobacco and *N. benthamiana*. For the selection of transgenic
149 progenies, seeds were disinfected by incubation under suspension in 10% trisodium phosphate
150 dodecahydrate for 20' and then in 3% sodium hypochlorite for 20'. Then, seeds were washed in sterile
151 distilled water and sown on germination medium (5 g/L MS with vitamins, 30 g/L sucrose, 9 g/L Phytoagar,
152 pH = 5.7) supplemented with 100 mg/L kanamycin for positive transgene selection. *NtLPPS-AAT4* tobacco
153 seeds were supplemented with both 100 mg/L kanamycin and 20 mg/L hygromycin for simultaneous
154 transgenic selection. Control plants were obtained similarly, by placing seeds on a non-selective germination
155 medium. WT and antibiotic-resistant seedlings were transferred to the greenhouse 15 days after
156 germination, where they were grown at 24 : 20°C (light : darkness) with a 16 : 8 h light :darkness photoperiod.
157 The segregation of transgenes and the estimation of transgene copy number were determined by calculating
158 survival percentages of seedlings germinated on selective media. Transgene copy number was estimated
159 using the Chi squared test. T₀ lines were assumed to be multiple copy lines for the transgene when
160 segregation of the transgene was not possible in the T₁ progeny, and no segregation was detected in the
161 following transgenic generations.

162 Plant sampling

163 Samples for VOCs analysis in the T₀, T₁ and T₂ generations were collected from the youngest fully expanded
164 leaves of 35-40 days-old *N. benthamiana* or *N. tabacum* plants using a Ø 1.5-2 cm corkborer and snap frozen
165 in liquid nitrogen.

166 For the analysis of T₃ *N. benthamiana* plants, the first collection of leaf tissue was performed just before the
167 first flower reached anthesis (-1 day), choosing the youngest leaves ranging in length from 3 to 5 cm

168 (henceforth named young leaves), and middle-stem fully expanded leaves (henceforth named adult leaves).
169 The second collection of leaf tissue (post-flowering stage) was carried out after 90 days in soil, following the
170 same criteria adopted in the first collection for the selection of young and adult leaves. For senescent leaves,
171 leaves in the lower part of the stem were sampled when turning slightly yellow. Three leaves per leaf type
172 were sampled as biological replicates.

173 For the analysis of T_3 *NtLPPS* and *NtCPPS* tobacco plants, and of T_1 *NtLPPS-AAT4* tobacco plants, leaf tissue
174 collection was performed just before the first flower reached anthesis (-1 day), sampling upper-stem leaves
175 ranging in length from 15 to 25 cm (henceforth named young leaves), middle-stem fully expanded and deep
176 green leaves (henceforth named adult leaves), and lower-stem leaves, turning slightly yellow, for senescent
177 leaves. Three leaves per leaf type were sampled as biological replicates.

178 For the biomass calculation and estimation of total plant production, four-month-old tobacco plants were
179 harvested at the end of the assay and their leaves classified according to leaf age; a correction factor based
180 on production levels measured at different leaf ages was used to estimate total yields.

181 *N. benthamiana* leaf samples for intact tissue HSPME VOCs analysis were collected from young leaves ranging
182 in weight from 150 to 350 mg and rolled inside the vials. Emission values were later normalized using leaf
183 weight. Tobacco leaf samples for volatile release in dynamic condition assays were represented by young
184 leaves from the upper part of the plant, 30-35 cm long.

185 Flower sampling was carried out at pre-anthesis (-1 day for *N. benthamiana*) and with completely open
186 flowers, for both *N. benthamiana* and *N. tabacum* flowers.

187 **Analysis of volatile organic compounds (VOCs)**

188 For powdered samples, 50 mg of frozen, ground leaf or flower tissue were weighed in a 10 mL or 20 mL
189 headspace screw-cap vial and stabilized by adding 1 mL of 5M CaCl_2 and 150 μL of 0.5 M EDTA, pH=7.5, after
190 which they were immediately bath-sonicated for 5'. Volatile compounds were captured by means of
191 headspace solid phase microextraction (HS-SPME) with a 65 μm polydimethylsiloxane/divinylbenzene
192 (PDMS/DVB) SPME fiber (Supelco, Bellefonte, PA, USA). Volatile extraction was performed automatically by
193 means of a CombiPAL autosampler (CTC Analytics, Zwingen, Switzerland).

194 For the T_0 , T_1 and T_2 generations in *N. benthamiana*, and for the T_0 and T_1 generations in *N. tabacum*, analyses
195 were made using a PEGASUS 4D mass spectrometer (LECO Corporation, St. Joseph, MI, USA). Vials were first
196 incubated at 50°C for 10' under 500 rpm agitation. The fiber was then exposed to the headspace of the vial
197 for 20' under the same conditions of temperature and agitation. Desorption was performed at 250°C for 1'
198 (splitless mode) in the injection port of a 6890 N gas chromatograph (Agilent Technologies, Santa Clara, CA,
199 USA) coupled to PEGASUS 4D mass spectrometer (LECO Corporation). After desorption, the fiber was cleaned
200 in a SPME fiber conditioning station (CTC Analytics) at 250°C for 5' under a helium flow. Chromatography was
201 performed on a BPX-35 (30 m, 0.32 mm, 0.25 μm) capillary column (SGE) with helium as the carrier gas at a
202 constant flow of 2 mL/min. The oven conditions started with an initial temperature of 40°C for 2', 5°C/min
203 ramp until 250°C, and a final hold at 250°C for 5'. Data was recorded in a PEGASUS 4D mass spectrometer
204 (LECO Corporation) in the 35-300 m/z range at 20 scans/s, with electronic impact ionization at 70 eV.
205 Chromatograms were processed by means of the ChromaTOF software (LECO Corporation).

206 For the T_3 generation *N. benthamiana* *LPPS* and *CPPS* transformants, the T_2 and T_3 generation tobacco *LPPS*
207 and *CPPS* transformants, and the T_0 and T_1 *LiLPPS LiAAT4* tobacco transformants, desorption was performed
208 at 250°C for 1' (splitless mode) in the injection port of a 6890 N gas chromatograph (Agilent Technologies)
209 coupled to a 5975B mass spectrometer (Agilent Technologies). Chromatography was performed on a DB5ms
210 (60 m, 0.25 mm, 1 μm) capillary column (J&W) with helium as the carrier gas at a constant flow of 1.2 mL/min.
211 Oven conditions were the same indicated above. Data was recorded in 5975B mass spectrometer in the 35-
212 300 m/z range at 20 scans/s, with electronic impact ionization at 70 eV. Chromatograms were processed by
213 means of the Agilent MassHunter software (Agilent Technologies).

214 For intact tissue assays, leaf or flower tissue samples were weighed and placed in a 20 mL headspace screw-
215 cap vial. Volatile compounds were captured by means of headspace solid phase microextraction (HS-SPME)

216 with a 65 μm polydimethylsiloxane/divinylbenzene (PDMS/DVB) SPME fiber (Supelco). Volatile extraction
217 was performed automatically by means of a CombiPAL autosampler (CTC Analytics). Vials were first incubated
218 at 30°C for 10' under 500 rpm agitation.

219 Chromatograms were processed by means of the Agilent MassHunter software. Identification of compounds
220 was made by comparison of both retention time and mass spectrum with pure standards (lavandulol,
221 chrysanthemol, linalool and lavandulyl acetate) and by comparison between mass spectrum for each
222 compound with those of the NIST 2017 spectral library. Every compound quantification was corrected with
223 the value of the daily deviation of a master mix, processed and analyzed every day. A linalool internal
224 standard (IS) was always added as a control of hour drift.

225 The quantification of monoterpene compounds emitted either by whole plants, or by detached leaves or
226 flowers was carried out by volatile collection in dynamic conditions. Individual plants for *N. benthamiana* or
227 50 g of tobacco leaves were placed inside 5 L glass reactors (25 cm high \times 17.5 cm diameter flask) with a 10
228 cm open mouth and a ground glass flange to fit the cover with a clamp. The cover had a 29/32 neck on top
229 to fit the head of a gas washing bottle and to connect a glass Pasteur pipette downstream to trap effluents
230 in 400mg of Porapak-Q 80-100 (Waters Corporation, Milford, MA, USA) adsorbent. For tobacco flowers,
231 around 3 g of flowers were placed inside 1.3 L glass chambers (50 cm length \times 6 cm diameter cylinder). Plant
232 and leaf samples were collected continuously for 72 h, and flower samples for 48 h, by using an ultrapurified-
233 air stream, provided by an air compressor (Jun-air Intl. A/S, Norresundby, Denmark) coupled with an AZ 2020
234 air purifier system (Claind Srl, Lenno, Italy) to provide ultrapure air (amount of total hydrocarbons < 0.1 ppm).
235 In front of each glass reactor, an ELL-FLOW digital flowmeter (Bronkhorst High-Tech BV, Ruurlo, The
236 Netherlands) was fitted to provide an air push flow of 100 mL/min during sampling. Volatiles trapped in the
237 Porapak Q cartridges were eluted with 3 mL pentane. Solvent extracts were concentrated under a gentle
238 nitrogen stream up to 500 μL and 25 μL of an internal standard solution (100 $\mu\text{g}/\text{mL}$ in dichloromethane)
239 were added to the sample prior to the chromatographic analysis for quantification of the target molecules.

240 **Solvent extraction from plant tissues**

241 The total quantity of pheromone compounds accumulated in each plant or leaf bunch was extracted with
242 toluene (TLN). Plant samples (ca. 3 g), mixed with fine washed sand (1 : 1, plant : sand, w/w), were manually
243 ground with a mortar to aid in tissue breakdown and facilitate the extraction. The resulting material was then
244 transferred to 50 mL centrifuge tubes with 10 mL TLN. The extraction process was assisted by magnetic
245 agitation for 12 h and finally by ultrasound in a Sonorex ultrasonic bath (Bandelin electronic, Berlin, Germany)
246 for 30'. A 1 mL sample of the resulting extract was filtered through a PTFE syringe filter (0.25 μm). Twenty-
247 five μL of an internal standard solution (100 $\mu\text{g}/\text{mL}$ in dichloromethane) were added to the sample prior to
248 the chromatographic analysis for quantification of the target molecules.

249 **Quantification of target compounds**

250 The quantification was performed by gas chromatography coupled to mass spectrometry (GC-MS), using an
251 internal standard. A straight chain fluorinated hydrocarbon ester (heptyl 4,4,5,5,6,6,7,7,8,8,9,9,9-
252 tridecafluorononanoate; TFN) was selected as the internal standard to improve both sensitivity and
253 selectivity for MS detection (Gavara et al. 2020).

254 One μL of each extract was injected in a Clarus 690 gas chromatograph (Perkin Elmer Inc., Wellesley, MA)
255 coupled to a Clarus SQ8T MS instrument operating in full scan mode and using EI (70 eV). The GC was
256 equipped with a ZB-5MS fused silica capillary column (30m \times 0.25mm i.d. \times 0.25 μm ; Phenomenex Inc.,
257 Torrance, CA). The oven was held at 60°C for 1 min then was raised by 10°C/min up to 120°C, maintained for
258 4 min, raised by 10°C/min up to 130°C, and finally raised by 20°C/min up to 280°C held for 2 min. The carrier
259 gas was helium at 1 mL/min. The GC injection port and transfer line were programmed at 250 °C, whereas
260 the temperature of the ionization source was set at 200°C. Chromatograms and spectra were recorded with
261 GC-MS Turbomass software version 6.1 (PerkinElmer Inc.).

262 The amount of each compound and the corresponding chromatographic areas were connected by fitting a
263 linear regression model, $y = a + bx$, where y is the ratio between compound and TFN areas and x is the amount
264 of compound.

265 **Chlorophyll Index measurements**

266 For T_3 generation *N. benthamiana* and *N. tabacum* LPPS and CPPS transformants, and T_1 NtLPPS-AAT4
267 tobacco transformants, chlorophyll index (C.I.) data were collected with a Dualex-A optical sensor (Dualex
268 Scientific® (Force-A, Orsay, France). Three leaves per plant were sampled for each leaf stage: young and adult
269 leaves in pre-flowering plants, and young, adult and early senescent leaves in post-flowering plants, using
270 the same criteria specified for plant sampling.

271 **Synthesis of pure standards for GC-MS**

272 **Linalool.** Standard sample of linalool was commercially acquired from Sigma-Aldrich.

273 **Racemic Lavandulol.** A solution of methyl acrylate (1.5 g, 0.013 mol) in dry tetrahydrofuran (5 ml) was slowly
274 added to a cooled solution of lithium diisopropylamide at $-40\text{ }^\circ\text{C}$ (2.0 M in THF, 7.9 ml, 1.2 eq) under nitrogen.
275 After 60 min of continuous stirring, prenyl bromide (2.22 g 0.014 mol, 1.15 eq) were added, and the solution
276 was warmed up to room temperature and stirred for an additional 5 h. The reaction was quenched by the
277 addition of saturated ammonium chloride solution (5 ml) and extracted with Et_2O (3 X 15 ml). The combined
278 organic phases were successively washed with HCl 1M (1 X 5 ml), NaHCO_3 10 % (1X 5 ml) and brine (1 X 10
279 ml), dried with anhydrous magnesium sulphate, and the solvent evaporated under vacuum. The crude
280 material was dissolved in anhydrous tetrahydrofuran (4 ml) and slowly added to a suspension of LiAlH_4 (0.67
281 g, 0.017 mol, 1.35 eq.) in dry THF (5 ml) at $0\text{ }^\circ\text{C}$ under argon atmosphere. After 3 h of continuous stirring,
282 sodium sulphate decahydrated (Glauber's salt) was carefully added to the suspension until a clear solid was
283 formed (hydrogen formed during the quenching was removed with a continuous stream of nitrogen). The
284 solid was filtered off through a celite pad, and the solvent evaporated under vacuum. The crude material was
285 purified by column chromatography using a mixture of hexane:acetate (8:2) as eluent. Evaporation of the
286 solvent of the corresponding fractions afforded pure lavandulol (1.4 g, 96 % purity by GC-FID, 70 % overall
287 yield for two steps). The spectroscopical properties of lavandulol were fully coincident with those described
288 in the literature (Pepper *et al.* 2014).

289 **Lavandulyl acetate.** Triethyl amine (1.05 ml, 7.6 mmol, 1.8 eq.) and acetic anhydride (0.46 ml, 4.8 mmol, 1.15
290 eq.) were subsequently added to a solution of lavandulol (0.65 g, 4.2 mmol) in dry dichloromethane (8 ml) at
291 room temperature. After 5 h of continuous stirring, the reaction was poured in dichloromethane (15 ml) and
292 subsequently washed with HCl 1M (1 X 10 ml), NaHCO_3 10 % (1X 10 ml) and brine (1 X 10 ml), dried with
293 anhydrous magnesium sulphate, and the solvent evaporated under vacuum. The crude material was purified
294 by column chromatography using a mixture of hexane:acetate (9:1) as eluent. Evaporation of the solvent of
295 the corresponding fractions afforded pure lavandulol (0.78 g, 98 % purity by GC-FID, 95 % yield). The
296 spectroscopical properties of lavandulol acetate were fully coincident with previously reported data (Cross
297 *et al.* 2004).

298 **Chrysantemol.** A solution of chrysanthemic acid (mixture of isomers, 3 g, 18 mmol) in anhydrous
299 tetrahydrofuran (6 ml) was slowly added to a suspension of LiAlH_4 (1.4 g, 38 mmol, 2 eq.) in dry THF (20 ml)
300 at $0\text{ }^\circ\text{C}$ under argon atmosphere. The reaction mixture was warm up to room temperature and, after 5 h of
301 continuous stirring, sodium sulphate heptahydrated (Glauber's salt) was carefully added to the suspension
302 until a clear solid was formed (hydrogen formed during the quenching was removed with a continuous
303 stream of nitrogen). The solid was filtered off through a celite pad, and the solvent evaporated under vacuum.
304 The crude material was purified by column chromatography using a mixture of hexane:acetate (7:3) as
305 eluent. Evaporation of the solvent of the corresponding fractions afforded pure (+)-*trans*-chrysanthemol (2.3
306 g, 96 % purity by GC-FID, 85 % yield). The spectroscopical properties of (+)-*trans*-chrysanthemol were fully
307 coincident with those described in the literature (Dufour *et al.* 2012).

308 **Statistical analysis**

309 Statistical analyses were performed using the Past4 software (Hammer *et al.*, 2001) and GraphPad Prism
310 v8.0.2 (GraphPad Software, San Diego, CA, USA).

311 Results

312 1. Volatile irregular monoterpene alcohols lavandulol and chrysanthemol are efficiently produced 313 in tobacco and *N. benthamiana*.

314 The production of irregular monoterpenoids from their DMAPP precursor (Figure 1A) in non-specialized leaf
315 cells was first assayed by transient agroinfiltration in *N. benthamiana* of the genes encoding the
316 corresponding isoprenyl transferases. The coding sequences of *LiLPPS* and *TcCPPS* were assembled in
317 separate GoldenBraid vectors, each of them regulated by the Cauliflower Mosaic Virus 35S promoter
318 (pCaMV35S) and the nopaline synthase terminator (tNOS) (Figure 1B,C). The volatile organic compound
319 (VOC) composition of infiltrated leaves was analyzed 5 days post-infiltration (dpi) by headspace solid-phase
320 micro-extraction (HS-SPME) gas chromatography/mass spectrometry (GC/MS). Production of the volatile
321 monoterpene alcohols lavandulol and chrysanthemol was successfully detected in *LiLPPS*- and *TcCPPS*-
322 agroinfiltrated samples, respectively (Figure 1B,C). Relative quantifications are shown in Figure 1E. None of
323 these products was detectable in negative controls (Figure 1D,E). In *TcCPPS*-infiltrated leaves other related
324 volatile monoterpenoids were detected, namely Artemisia and Yomogi alcohols and santolinatriene, as
325 identified by the NIST mass spectral library (2017). Both Artemisia and Yomogi alcohol are known to derive
326 from the chrysanthemyl cation in aqueous environments, through the rupture of its C(1')-C(3') cyclopropane
327 bond (Poulter *et al.*, 1977; Rivera *et al.*, 2001).

328 Given the success obtained in transient expression, the generation of stable lines producing lavandulol and
329 chrysanthemol was attempted both for *N. benthamiana* and tobacco. Twelve T₀ *LiLPPS N. benthamiana*
330 (*NbLPPS*) plants and four T₀ *LiLPPS* tobacco (*NtLPPS*) plants were recovered on selective media. Similarly,
331 seven *TcCPPS N. benthamiana* (*NbCPPS*) and three *TcCPPS* tobacco (*NtCPPS*) T₀ plants were obtained. The
332 production of targeted monoterpenoids in all four transformation experiments was followed for individual
333 plants in T₀, T₁ and T₂ generations, and the results are shown in Figure S1. Selection for best-performing lines
334 through generations was made based on production/growth balance, and general trends remained stable up
335 to the T₂ generation. *NtLPPS* plants (especially line *NtLPPS_3_1*) were more productive than their *N.*
336 *benthamiana* counterparts, with up to 7-fold the lavandulol levels detected in *NbLPPS* plants, except for line
337 *NbLPPS_11_2_4*, whose levels reached 50% those of the best tobacco producers. *NtCPPS* plants produced
338 over 4 times more chrysanthemol than their *NbCPPS* counterparts. In both species, plants producing
339 lavandulol showed yellowing and slower growth, in contrast to non-producer transgenic plants, which were
340 comparable to WT, and a similar trend was observed for *NbCPPS* and *NtCPPS* plants. Especially for *NbCPPS*
341 and *NtCPPS*, production was associated with premature blossom drop and frequent failure to reach fruit set
342 (not shown). In all chrysanthemol-producing plants, the derived products Artemisia and Yomogi alcohols and
343 santolinatriene were detected, most likely being breakdown products generated during sample processing
344 (Figure S2). This points to a likely under-estimation of chrysanthemol in these samples. However, while taking
345 this factor into consideration, at this point we used these assays only as relative quantification methods to
346 compare different plants within the *NbCPPS* and *NtCPPS* populations.

348 2. Lavandulol and chrysanthemol production is higher in the earlier developmental stages and in 349 young leaves of *N. benthamiana* and tobacco transgenic lines

350 For a thorough characterization of transgenic *N. benthamiana* and tobacco plants, we analyzed the levels of
351 the target compounds in leaves at different developmental stages of the plant, as well as at different stages
352 of leaf development, in a uniform T₃ generation. Two tobacco (*NtLPPS_1_3_2* and *NtLPPS_3_1_3*) and two
353 *N. benthamiana* (*NbLPPS_11_2_4* and *NbLPPS_5_2_2*) lines were selected based on their lavandulol
354 production levels. For *NbCPPS* and *NtCPPS*, one vigorous line with a single T-DNA insertion, characterized by
355 high production rates, was selected for each *Nicotiana* species. Overexpression of monoterpenes is known
356 to affect plant growth and fertility, a trend we had observed in the T₁ and T₂ generations of plants producing
357 lavandulol and chrysanthemol. As expected, all T₃ transgenic lines showed a delay in flowering time compared

358 to WTs (Figure 2A,E). This delay consists of a 20-30% increase in the number of days in soil before flowering
359 in *N. benthamiana*, while in tobacco the delay can be greater, reaching 93% in *NtLPPS_3_1_3*. No significant
360 differences between genotypes are found regarding plant height except for *NtLPPS_3_1_3* (Figure 2B,F), but
361 a reduction in biomass is observed. In *N. benthamiana*, both *NbLPPS* lines show a significant reduction in
362 biomass (estimated as FW after 100 days in soil) which can range between 60 and 80% compared to both WT
363 and *NbCPPS* (Figure 2C,D). In tobacco, differences in size and plant biomass are not significant between WT
364 and *NtCPPS*, but they are for *NtLPPS*, whose biomass is reduced between 35 and 75% (Figure 2G,H). The
365 chlorophyll index (C.I.) is another parameter for measuring loss of fitness due to overexpression of
366 monoterpenoids, since these compounds often induce chlorosis. In *N. benthamiana*, no significant
367 differences are found in the C.I. of *NbCPPS* compared to WTs, while for *NbLPPS* there is a reduction at both
368 the pre- and post-flowering stages (Figure S3). In tobacco, both *NtLPPS* and *NtCPPS* show a reduction in C.I.
369 at the pre-flowering stage, which disappears post-flowering (Figure S3). In all cases, differences correlate
370 with higher monoterpenoid production (see also Figure 3). No correlation was found between the number
371 of copies of the transgene and production levels or other phenotypic effects. According to segregation
372 patterns, *NbLPPS_11_2_4* and *NtLPPS_1_3_2* had a single T-DNA insertion, while *NbLPPS_5_2_2* and
373 *NtLPPS_3_1_3* carried multiple transgene copies. While plants of the multiple-copy line *NtLPPS_3_1_3* show
374 the most severe pleiotropic effects, in *N. benthamiana* the single-copy line *NbLPPS_11_2_4* has the greatest
375 yields and most severe phenotypes.

376 The monoterpenoid content of leaves was assessed pre- and post-anthesis in *N. benthamiana* plants. Pre-
377 anthesis, two types of leaves were analyzed (Y=young and A=adult), while post-anthesis a third type of leaf
378 (S=senescent) was included. The analysis of the monoterpenoid content in different individuals and tissues
379 (Figure 3A,B and Data File S1) shows that the factor affecting productivity the most is the type of tissue. Plants
380 within each line show homogeneous phenotypes in terms of production levels and fitness, and no significant
381 differences are found between plants descending from the same T₂ parental. Overall, young leaves of pre-
382 anthesis plants are the most productive vegetative tissues in both *NbLPPS* and *NbCPPS* lines, followed by the
383 adult leaves of these pre-anthesis plants (Figure 3A,B). We observed a decrease in the levels of the target
384 monoterpenoids in fully flowering plants, diminishing with the increase in leaf age (Figure 3A,B). In *NbLPPS*
385 and *NbCPPS*, adult leaves of pre-flowering plants and young leaves of post-anthesis plants usually show
386 similar production levels. Senescent leaves are still productive, even if a clear decline was observed for all
387 analyzed compounds. In tobacco, only one sampling was performed just prior to anthesis, and three leaf
388 types were collected (Y=young, A=adult and S=senescent). The same decrease in monoterpenoid production
389 with increasing leaf age was identified in *NtLPPS* and *NtCPPS* plants: young leaves stand out as the most
390 productive vegetative tissue in tobacco (Figure 3C,D and Data File S1). *NbLPPS_11_2_4* and *NtLPPS_3_1_3*
391 have comparable levels of lavandulol, especially in young leaves. By contrast, tobacco produced more
392 chrysanthemol than *N. benthamiana*, with young leaves of *NtCPPS_1_3_2* producing more than twice the
393 levels detected in the best performing *NbCPPS_5_4_1* young pre-flowering leaves.

394 For a more accurate measure of monoterpenoid production, solvent extraction was used to obtain absolute
395 quantifications; for this, materials from the best-yielding conditions and single copy lines were analyzed.
396 From *NbLPPS_11_2_4* whole young T₃ plants, almost 35 µg/g FW of lavandulol were obtained, in contrast to
397 0.6 µg/g FW of chrysanthemol in *NbCPPS_5_4_1* plants (Table 1). These quantifications correlate with the
398 accumulation of lavandulol and chrysanthemol observed in relative quantifications (Figure 3A,B). A similar
399 trend was observed in tobacco: an average of 22.55 µg/g FW of lavandulol were retrieved from young leaves
400 of *NtLPPS_1_3_1* plants, while extraction from young leaves of *NtCPPS_1_3_2* plants yielded an average of
401 0.6 µg/g FW of chrysanthemol (Figure 3C,D and Table 1).

402 3. The potential for volatilization of lavandulol and chrysanthemol in vegetative and reproductive 403 tissues of transgenic lines

404 Volatilization from stabilized ground tissue in HSPME vials was adopted as a high-throughput screening
405 method to estimate the content of VOCs, requiring minimal amounts of manipulation and reagents, which
406 allowed us to compare a great number of samples in parallel, while also getting a general picture of the tissue
407 volatilome beyond extraction of single classes of compounds. Other approaches (in addition to solvent
408 extraction) were deemed necessary to characterize the production and emission of monoterpenoid alcohols
409 more accurately, keeping in mind the prospective use of plants as live bio-dispensers. Two strategies were
410 followed: *i*) incubating intact samples in HSPME vials and analyzing the emitted compounds and *ii*) analyzing
411 volatiles emitted by intact plants or leaves under dynamic conditions. Flowers emit great quantities of
412 volatiles in many plant species (Loughrin *et al.*, 1991; Dudareva *et al.*, 2013; Adebessin *et al.*, 2017): we
413 wondered if *N. benthamiana* or tobacco flowers could be responsible for a considerable percentage of the
414 total volatile monoterpenoid production of our transgenic plants. In addition to leaves, both intact and
415 ground flowers from transgenic plants were analyzed by HSPME GC/MS.

416 For *NbLPPS*, the lavandulol emitted by intact leaves represented around one eighth of the lavandulol
417 measured in homogenized samples (Figure 4A). The lavandulol detected in ground *NbLPPS* flowers is 22% of
418 that of ground leaves, but the volatilized portion is higher in flowers, with the emitted fraction reaching
419 almost 30% of that measured in ground flower samples (Figure 4A). Lavandulol emission was similar when
420 intact flowers and leaves were compared. An analogous trend was observed for *NbCPPS*: chrysanthemol
421 emission was almost undetectable in intact leaves, while being considerably higher in ground tissue (Figure
422 4B), and it was also detected in intact flowers, which emit around 90% more chrysanthemol than leaves per
423 biomass unit. The production of lavandulol and chrysanthemol did not depend on the developmental stage
424 of *N. benthamiana* flowers, since no differences were found between flowers before and after anthesis for
425 either compound (Figure S4). When quantifying emission from young intact *N. benthamiana* plants under
426 dynamic conditions, 160 ng/g FW/day lavandulol were detected in *NbLPPS* plants, four times the amount of
427 chrysanthemol emitted by *NbCPPS* plants (40 ng/g FW/day, Table 2).

428 In tobacco transgenic lines, lavandulol and chrysanthemol are produced at comparable levels in ground
429 flowers and young leaves (Figure 4C,D). In terms of volatility, flowers emit 5.6 times more lavandulol than
430 leaves per biomass unit, while no significant differences are found for chrysanthemol between the two
431 tissues (Table 2). Comparing emission of lavandulol and chrysanthemol, under dynamic conditions the
432 lavandulol released by *NtLPPS* young leaves (53.89 ng/g FW/day) is almost three times more abundant than
433 the chrysanthemol released by *NtCPPS* leaves (18.1 ng/g FW/day). Again, flowers proved to be better
434 emitters than leaves: *NtLPPS* flowers released almost six-fold more lavandulol than vegetative tissues of the
435 same biomass, and *NtCPPS* flowers almost doubled the chrysanthemol emission of the leaves (Table 2).

436 Comparing the two biofactories, monoterpenoid alcohol levels are similar in ground floral tissues, but the
437 potential for emission is greater in tobacco than in *N. benthamiana* flowers. Compared to *NbLPPS*, *NtLPPS*
438 leaves emitted one third of the lavandulol volatilized by *NbLPPS* whole plants; similarly, *NtCPPS* leaves
439 emitted around half of the chrysanthemol released by *NbCPPS* whole plants, per biomass unit (Table 2). The
440 two sets of values are not fully comparable (whole plants vs. detached leaves), yet we can hypothesize that,
441 considering the production levels estimated for the different kind of leaves, the greater biomass of adult
442 tobacco plants would allow a considerably greater total emission. Interestingly, the chrysanthemol-derived
443 compounds Artemisia and Yomogi alcohols found in ground samples are barely detectable, if at all, in the
444 emitted volatilome of intact samples (Data File S2).

445 4. Lavandulol can be esterified to lavandulyl acetate by the *LiAAT-4* acetyltransferase in 446 tobacco

447 We wanted to test the ability of our plants to produce lavandulyl acetate as an example of an active
448 pheromone compound derived from one of the assayed precursors. In addition to its value as a fragrance,

449 (R)-lavandulyl acetate is a semiochemical found in the aggregation pheromone of the thrips *F. occidentalis*
450 (Hamilton *et al.*, 2005) and in the sex pheromone of the mealybug *D. grassii* (De Alfonso *et al.*, 2012). Notably,
451 Govindarajan & Benelli (2016) also highlighted its effectiveness as a mosquito larvicide with a LC50 of around
452 4 µg/ml in aqueous solution. The AAT4 acetyltransferase from *L. intermedia* (*LiAAT4*) acetylates
453 monoterpenoid alcohols, including lavandulol (Sarker & Mahmoud, 2015). We first tested *LiAAT4* in *N.*
454 *benthamiana* leaves: a construct containing the P35S::*LiAAT4*::*tNOS* transcriptional unit was agroinfiltrated
455 on T₃ *NbLPPS* plants (Figure 5A) and high levels of acetylation of the lavandulol substrate were obtained
456 (Figure 5B), with an average 70% of the substrate detected in the absence of *LiAAT4* converted to lavandulyl
457 acetate.

458 Given the greater biomass and general robustness of tobacco compared to *N. benthamiana*, we used the T₁
459 tobacco line producing the highest levels of lavandulol, *NtLPPS_3_1*, for stable transformation with *LiAAT4*.
460 In the *NtLPPS_AAT4* T₀ population, different efficiencies were observed for the conversion of lavandulol to
461 lavandulyl acetate, measured by HSPME GC-MS (Figure S5). Some individuals showed especially good
462 acetylation rates, producing levels of lavandulyl acetate comparable to those of lavandulol in their parental
463 line, with accordingly lower levels of lavandulol. However, a strong negative correlation was observed
464 between production levels and fitness, and the plants with the highest lavandulyl acetate production were
465 not able to produce viable seeds. For phenotypic characterization, the progeny of the plant with the highest
466 production levels which allowed to collect viable seeds (*NtLPPS_AAT4_8*) was chosen. As for *NtLPPS* plants,
467 we evaluated accumulation in different plant tissues. Like in T₃ tobacco and *N. benthamiana* plants producing
468 lavandulol and chrysanthemol, young leaves of T₁ *NtLPPS-AAT4* plants were the most productive tissues
469 (between 2- and 7-fold more than adult leaves), while the lowest levels of lavandulyl acetate were observed
470 in senescent leaves, paralleling lavandulol availability (Figure 5C). Again, the greatest source of variation was
471 the type of tissue. No significant differences were found between the levels of lavandulyl acetate in the three
472 tested T₁ individuals within each leaf type, while *NtLPPS-AAT4_8_4* accumulated more alcohol in young and
473 adult leaves than the other T₁ plants. Considering the total monoterpenoid content of the three individuals,
474 no significant differences were found. The same analyses performed for *NtLPPS* and *NtCPPS* were carried out
475 on *NtLPPS-AAT4* to determine production and emission in flowers and leaves and to quantify lavandulyl
476 acetate by solvent extraction and under dynamic conditions. In absolute quantifications following solvent
477 extraction, lavandulyl acetate appeared to be less accumulated in leaf tissues than lavandulol (Table 3). These
478 data contrast sharply with the results of the analyses of homogenized tissue, in which the acetate:alcohol
479 ratio is always higher and favors the acetate (Figure 5C), making us wonder whether part of it might be lost
480 during the extraction procedure. As for *in vivo* release from leaves under dynamic conditions, volatilization
481 is higher for lavandulyl acetate than for lavandulol: the highest producing plants release on average 626.84
482 ng/g FW/day of lavandulyl acetate and 72.45 ng/g FW/day of lavandulol (Table 4), compared to 53.89 ng/g
483 FW/day of lavandulol released by the *NtLPPS_1_3_1* parental line (Table 2). Regarding flowers, in
484 homogenized samples lavandulol and lavandulyl acetate levels are remarkably similar (Figure 5D), also being
485 comparable to those of lavandulol in *NtLPPS* flowers (Figure 4C). Volatilization from intact flowers favors
486 lavandulyl acetate over lavandulol, although in absolute terms the emission rate from flowers is on average
487 2.5-fold less abundant than it is from young leaves (253 vs 627 ng/gFW/day, see Table 4). The heterologous
488 production of lavandulyl acetate, too, was accompanied by pleiotropic effects such as yellowing leaves, a
489 delay in flowering and a lower biomass at flowering time (Figure 5E,F,G,H and Figure S3). Interestingly, when
490 compared to the T₃ tobacco plants derived from the same parental used for stacking the *LiAAT4* transgene,
491 the phenotype of the plants producing only lavandulol (Figure 2H) was overall more severe than that of those
492 producing high levels of lavandulyl acetate: *NtLPPS_3_1_3* plants accumulate 22% of the leaf biomass of WT
493 tobacco, while *NtLPPS_AAT4_8* T₁ plants reach 53%. However, the greatest reduction in chlorophyll index
494 was found in *NtLPPS-AAT4* plants (Figure S3).

495 Discussion

496 In this study, we demonstrated the potential of tobacco and *N. benthamiana* plants as biofactories of
497 irregular monoterpenes and their derivatives. Several reports show the heterologous production of mono-
498 and sesquiterpenes in bacteria, yeasts and plants (Q. Wang *et al.*, 2019; Xie *et al.*, 2019; Dusséaux *et al.*, 2020;
499 Fuentes *et al.*, 2016). However, very few examples exist of the production of irregular monoterpenoids, and
500 many of their biosynthetic pathways remain unknown (Minteguiaga *et al.*, 2023). The most widely studied
501 among irregular monoterpene derivatives is chrysanthemol, for its importance as the monoterpene
502 moiety of type I pyrethrins. Its full biosynthetic pathway was elucidated (Xu, Moghe, *et al.*, 2018) and
503 heterologous expression was achieved in fruits and glandular trichomes of tomato (Xu, Lybrand, *et al.*, 2018;
504 Wang *et al.*, 2022). Yang *et al.* (2014) also expressed *TcCPPS* in tobacco to demonstrate its ability to produce
505 chrysanthemol *in planta*, but this was done mainly as a proof of concept rather than to estimate the yield of
506 tobacco biofactories. Concomitantly, heterologous production of insect pheromones has focused almost
507 exclusively on moth sex pheromones, with a few notable exceptions, like the production of 8-hydroxygeraniol
508 in engineered yeast (H. Wang *et al.*, 2022), and that of the sesquiterpenoid aphid alarm pheromone (*E*)- β -
509 farnesene in wheat, the first crop engineered to release an insect pheromone (Bruce *et al.*, 2015). In this
510 respect, our work moves towards filling this niche and establishing plant-based biofactories for irregular
511 monoterpenoids with prospective uses for extraction and formulation of a variety of products, as well as for
512 live emission in greenhouses or the open field. In this line, we focused on understanding the phenotypic
513 effects associated with bioproduction in unspecialized cells following a constitutive expression strategy, as
514 well as in estimating the biosynthetic potential.

515 Bioproduction of monoterpenes in *Nicotiana* using a constitutive overexpression strategy is not
516 physiologically innocuous. For instance, Yin *et al.* (2017) found early flowering and increased branching when
517 overexpressing the peppermint geranyl diphosphate synthase small subunit in tobacco. Other deleterious
518 effects were observed for different terpenoids, including chlorosis, dwarfism, and a reduction in fertility
519 (Huchelmann *et al.*, 2017). Because of the similarity of the phenotypes observed in different reports,
520 cytotoxicity of the new metabolites is considered not to be the only cause, and perhaps plant depletion of its
521 essential terpenoid precursors (IPP/DMAPP) is also playing a role. Many of the observed deleterious effects
522 in our transgenic plants were dose dependent. We observed a reduction in size and leaf biomass of transgenic
523 plants producing lavandulol and lavandulyl acetate, correlating with the greatest reductions in chlorophyll
524 index. In *N. benthamiana*, the reduction in leaf biomass for *NbLPPS* was due mostly to the observed reduction
525 in number of lateral shoots (data not shown). Despite the observed effects, in general plants showing
526 moderate production levels (e.g., chrysanthemol producers in this study) also showed moderate phenotypic
527 effects, suggesting that a balance between volatile productivity and biomass production can be reached.
528 Whether such balance is favorable in technoeconomic terms will depend on the absolute production levels
529 and the concentrations required for achieving a biological effect.

530 The analysis of productivity across tissues and developmental stages was useful to understand the dynamics
531 of biosynthesis, as well as the design of the best conditions for biofactory use. Metabolite accumulation
532 depends, at least in part, on precursor availability at a specific growth stage and on the activation of
533 competing metabolic pathways (Drapal *et al.*, 2021). Developmental information is also crucial to determine
534 at what stage plant tissues should be harvested or used as bio dispenser to maximize product yield. We found
535 that young leaves at the flowering stage are most productive tissue in most instances. We also observed that,
536 at least in the constitutive overexpression strategy followed here, flowers do not provide a special advantage
537 in terms of accumulation or volatile emission. In the light of these results, it could be advisable to grow plants
538 in short cycles, harvesting before flowering to maximize productivity. Also, non-flowering tobacco varieties
539 (Schmidt *et al.*, 2020) could be suitable biofactory candidates, especially as bio-emitters, since genetically
540 impeded flowering would not affect bioproduction negatively and would increase the biosafety profile. Other
541 suggested strategies to increase product yields and to reduce pleiotropic effects in heterologous hosts

542 include accumulation in trichomes using specific promoters and transporters (Huchelmann *et al.*, 2017). This
543 might not represent an ideal solution for the accumulation of volatile compounds in tobacco, since it does
544 not possess peltate trichomes such as those of aromatic plants, but rather, its capitate trichomes are
545 specialized for the secretion on the leaf surface of non-volatile diterpenes and phytoalexins (Tissier *et al.*,
546 2017). While it might be a worthwhile approach to increase volatilization for bioemitters, it is possible that
547 the greater mesophyll biomass still guarantees greater yields using ubiquitous promoters, given that fitness
548 loss is kept within acceptable levels.

549 As expected, absolute product yields were found to be metabolite dependent. Lavandulol yields were
550 consistently higher than those of chrysanthemol (38- and 58-fold more lavandulol than chrysanthemol was
551 extracted from tobacco and *N. benthamiana* tissues, respectively). Previous reports of heterologous
552 expression of *TcCPPS* found that chrysanthemol may be glycosylated (Xu, Lybrand, *et al.*, 2018) and this could
553 account for these consistently lower levels, as well as, possibly, for the lower fitness loss observed in *NbCPPS*
554 and *NtCPPS* plants. Based on the biomass data and the quantification of monoterpenoids, we could estimate
555 the average production per plant for each transgenic line as 0.3 mg chrysanthemol in *NtCPPS* plants, around
556 16 mg lavandulol for *NtLPPS* plants, and around 3.4 mg lavandulol from a *NtLPPS-AAT4* plant. For lavandulyl
557 acetate, only 0.20 mg of compound per plant could be extracted. It is important to note that the lavandulyl
558 acetate figure is probably underestimating the actual levels of metabolite accumulated in leaves due to
559 partial losses with toluene extraction method. As pointed out, relative quantifications using ground tissue
560 suggest higher contents: lavandulyl acetate was twice the lavandulol detected in *NtLPPS-AAT4_8* plants, and
561 also twice the lavandulol detected in *NtLPPS_1_3_1* plants. Alternative strategies for the extraction of
562 lavandulyl acetate based on different solvents or on collection and subsequent extraction of the emitted
563 volatiles could be assayed. Based on toluene extraction levels, approximately 6 kg of young tobacco leaves
564 (6 plants) would be necessary to produce enough lavandulyl acetate to treat 1 L of water against mosquito
565 larvae at its LC50 (Govindarajan & Benelli, 2016). Altogether, it seems clear that at the extractable yields
566 obtained using constitutive overexpression are currently too low to provide a competitive advantage to
567 alternative production systems.

568 In contrast with the modest technoeconomic perspectives of the constitutive expression strategy in terms of
569 extraction yields, our data suggests a high potential of the tobacco platform as volatile live biodispensers.
570 For this, it is important to put the data obtained here in the context of pest control strategies conducted in
571 the field with related pheromones. Comprehensive assessments of mating disruption strategies to control
572 the mealybug *Planococcus ficus* using lavandulyl senecioate were recently reported by Daane *et al.* (2020)
573 and Lucchi *et al.* (2019) using field deployed dispensers containing chemically synthesized racemic
574 compounds. Here it was found that significant results in pest control were obtained with dispensers loaded
575 with a total of 4.15 g/ha over a season. Likely, the conclusions drawn in these studies may apply to other
576 mealybugs and other pheromones comprising irregular monoterpene esters. According to our daily emission
577 estimations of lavandulyl acetate in tobacco plants (correcting for leaf age and number of leaves at each
578 stage in an adult plant), a few hundred (200-500) plants per hectare would be sufficient to ensure similar
579 release levels as those reported by Lucchi *et al.* (2019). Depending on the crop to which they would be
580 coupled, this might represent a feasible density. The factors relevant for the effectiveness of pheromone
581 dispensers include a steady emission rate (which can be more important than absolute pheromone
582 concentration) and constant coverage during the season, to ensure pheromone emission during all periods
583 of peak flight activity. Plant bioemitters, in this respect, represent interesting solutions because their
584 emission depends on renewable metabolic resources, and it is not restricted to the initial load of the
585 dispenser. The life cycle of a tobacco plant, for example, is compatible with that of other crops to which it
586 may be coupled as producer of pheromones. Also, all available dispensers use racemic mixtures, only half of
587 which is the active ingredient, while biosynthesis ensures stereospecificity.

588 In conclusion, we show here that tobacco plants producing irregular monoterpenoids, and particularly
589 lavandulyl acetate, are a valuable model to understand the feasibility of using live pheromone emitter plants
590 as tools for mating disruption. Further improvements might be envisioned to increase productivity and
591 volatilization. However, compared to previous works on plant-based production of lepidopteran pheromones
592 (Mateos-Fernández *et al.*, 2021), tobacco plants producing monoterpene esters appear to be a more viable
593 tool for plant-based pest control. Finally, in addition to being biofactories and live emitters, these plants
594 represent a versatile metabolic and genetic tool for the combinatorial assessment of a variety of enzymatic
595 activities (e.g., acyltransferases from different sources) acting upon the constitutively expressed
596 monoterpene precursors to yield an array of pheromone compounds and other bioactive molecules.

597 **Supplementary Data**

598 Supplementary Table S1. List of the GB constructs used or generated in this study.

599 Supplementary Figure S1. Stable production of lavandulol and chrysanthemol in transgenic *N. benthamiana*
600 and tobacco T0 – T2 plants.

601 Supplementary Figure S2. Levels of Artemisia alcohol, Yomogi alcohol and santolinatriene detected in
602 transgenic *TcCPPS N. benthamiana* and tobacco T0 – T2 plants.

603 Supplementary Figure S3. Chlorophyll Index (C.I.) of transgenic *N. benthamiana* and tobacco plants producing
604 irregular monoterpenoids.

605 Supplementary Figure S4. Production of volatile monoterpenoids in transgenic *N. benthamiana* T3 lines in
606 flowers at different development stages.

607 Supplementary Data File S1. All data and statistical analysis relative to figures in the main text.

608 Supplementary Data File S2. All data and statistical analysis relative to supplementary figures.

609 **Acknowledgments**

610 We thank Prof. Heribert Warzecha and Elisabeth Haumann from the Technical University of Darmstadt
611 (TUDA), for giving us the sequences of *LiLPPS* and *TcCPPS*. We also wish to thank Dr. Ana Espinosa-Ruiz and
612 Teresa Caballero-Vizcaino at the IBMCP metabolomic facility for their help with GC-MS assays.

613 **Author contributions**

614 RMF: conceptualization, investigation, writing – original draft preparation; SV: investigation, writing – review
615 and editing; INF: investigation, writing – review and editing; VNL: investigation, writing – review and editing;
616 DO: conceptualization, funding acquisition, writing – original draft preparation; SG: conceptualization,
617 investigation, supervision, writing – original draft preparation. All authors read and approved the final text.

618 **Conflict of interest**

619 The authors declare no conflict of interest.

620 **Funding statements**

621 This work received support from the European Research Area Cofund Action ‘ERACoBioTech’ SUSPHIRE
622 project (Sustainable Production of Pheromones for Insect Pest Control in Agriculture, grant agreement No.
623 722361), and by the PHEROPLUS grant (PLEC2021-008020) by the Spanish Ministry of Science and Innovation,
624 the Next Generation EU initiative and the Spanish Agencia Estatal de Investigación (AEI).

625 RMF acknowledges a PhD grant (ACIF/2019/226) from the Generalitat Valenciana. SG acknowledges a
626 postdoctoral grant (CIAPOS/2021/316) from the Generalitat Valenciana and the European Social Fund.

627 **Data availability**

628 All data reported in this study, as well as statistical analyses, is available in Supplementary Files S1 and S2,
629 deposited at Zenodo: <https://doi.org/10.5281/zenodo.8208703>. The sequences of the plasmids used for
630 transformation can be consulted at www.gbcloning.upv.es.

631

632

633 Bibliography

- 634 Adebessin, F., Widhalm, J. R., Boachon, B., Lefèvre, F., Pierman, B., Lynch, J. H., Alam, I., Junqueira, B., Benke,
635 R., Ray, S., Porter, J. A., Yanagisawa, M., Wetzstein, H. Y., Morgan, J. A., Boutry, M., Schuurink, R. C., &
636 Dudareva, N. (2017). Emission of volatile organic compounds from petunia flowers is facilitated by an ABC
637 transporter. *Science*, 356(6345), 1386–1388. <https://doi.org/10.1126/science.aan0826>
- 638 Bento, J. M. S., Parra, J. R. P., de Miranda, S. H. G., Adami, A. C. O., Vilela, E. F., & Leal, W. S. (2016). How
639 much is a pheromone worth? *F1000Research*, 5. <https://doi.org/10.12688/F1000RESEARCH.9195.1>
- 640 Bruce, T. J. A., Aradóttir, G. I., Smart, L. E., Martin, J. L., Caulfield, J. C., Doherty, A., Sparks, C. A., Woodcock,
641 C. M., Birkett, M. A., Napier, J. A., Jones, H. D., & Pickett, J. A. (2015). The first crop plant genetically
642 engineered to release an insect pheromone for defence. *Scientific Reports*, 5.
643 <https://doi.org/10.1038/srep11183>
- 644 Cross, H., Marriott, R., & Grogan, G. (2004). Enzymatic esterification of lavandulol—a partial kinetic resolution
645 of (S)-lavandulol and preparation of optically enriched (R)-lavandulyl acetate. *Biotechnology letters*, 26, 457-
646 460. <https://doi.org/10.1023/b:bile.0000018268.42802.d0>
- 647 Daane, K.M., Yokota, G.Y., Walton, V.M., Hogg, B.N., Cooper, M.L., Bentley, W.J., and Millar, J.G. (2020).
648 Development of a mating disruption program for a mealybug, *Planococcus ficus*, in vineyards. *Insects*, (2020),
649 1-20, 11(9). <https://www.mdpi.com/2075-4450/11/9/635>
- 650 De Alfonso, I., Hernandez, E., Velazquez, Y., Navarro, I., & Primo, J. (2012). Identification of the sex
651 pheromone of the mealybug *Dysmicoccus grassii* Leonardi. *Journal of Agricultural and Food Chemistry*,
652 60(48), 12959–12964. <https://doi.org/10.1021/jf304065d>
- 653 Demissie, Z. A., Erland, L. A. E., Rheault, M. R., & Mahmoud, S. S. (2013). The biosynthetic origin of irregular
654 monoterpenes in *Lavandula*: Isolation and biochemical characterization of a novel cis-prenyl diphosphate
655 synthase gene, lavandulyl diphosphate synthase. *Journal of Biological Chemistry*, 288(9), 6333–6341.
656 <https://doi.org/10.1074/jbc.M112.431171>
- 657 Ding, B. J., Hofvander, P., Wang, H. L., Durrett, T. P., Stymne, S., & Löfstedt, C. (2014). A plant factory for
658 moth pheromone production. *Nature Communications*, 5. <https://doi.org/10.1038/ncomms4353>
- 659 Drapal, M., Enfissi, E. M. A., & Fraser, P. D. (2021). Metabolic changes in leaves of *N. tabacum* and *N.*
660 *benthiana* during plant development. *Journal of Plant Physiology*, 265.
661 <https://doi.org/10.1016/j.jplph.2021.153486>
- 662 Dudareva, N., Klempien, A., Muhlemann, J. K., & Kaplan, I. (2013). Biosynthesis, function and metabolic
663 engineering of plant volatile organic compounds. *New Phytologist*, Vol. 198, Issue 1, pp. 16–32.
664 <https://doi.org/10.1111/nph.12145>
- 665 Dufour, S., Castets, P., Pickett, J. A., & Hooper, A. M. (2012). A diastereoselective synthesis of (1SR, 3SR, 7RS)-
666 3-methyl- α -himachalene, the sex pheromone of the sandfly, *Lutzomyia longipalpis* (Diptera: Psychodidae).
667 *Tetrahedron*, 68(25), 5102-5108. <https://doi.org/10.1016/j.tet.2012.04.037>
- 668 Dusséaux, S., Thomas Wajn, W., Liu, Y., Ignea, C., & Kampranis, S. C. (2020). *Transforming yeast peroxisomes*
669 *into microfactories for the efficient production of high-value isoprenoids*.
670 <https://doi.org/10.1073/pnas.2013968117>
- 671 Fuentes, P., Zhou, F., Erban, A., Karcher, D., Kopka, J., & Bock, R. (2016). *A new synthetic biology approach*
672 *allows transfer of an entire metabolic pathway from a medicinal plant to a biomass crop*.
673 <https://doi.org/10.7554/eLife.13664.001>

- 674 Garabagi, F., Gilbert, E., Loos, A., Mclean, M. D., & Hall, J. C. (2012). Utility of the P19 suppressor of gene-
675 silencing protein for production of therapeutic antibodies in *Nicotiana* expression hosts. *Plant Biotechnology*
676 *Journal*, 10(9), 1118–1128. <https://doi.org/10.1111/j.1467-7652.2012.00742.x>
- 677 Gavara, A., Vacas, S., Navarro, I., Primo, J., and Navarro-Llopis, V. (2020). Airborne pheromone quantification
678 in treated vineyards with different mating disruption dispensers against *Lobesia botrana*. *Insects*, 11(5), 289;
679 <https://doi.org/10.3390/insects11050289>
- 680 Gerasymenko, I., Sheludko, Y. V., Navarro Fuertes, I., Schmidts, V., Steinel, L., Haumann, E., & Warzecha, H.
681 (2022). Engineering of a Plant Isoprenyl Diphosphate Synthase for Development of Irregular Coupling
682 Activity. *ChemBioChem*, 23(1). <https://doi.org/10.1002/cbic.202100465>
- 683 Govindarajan, M., & Benelli, G. (2016). Eco-friendly larvicides from Indian plants: Effectiveness of lavandulyl
684 acetate and bicyclogermacrene on malaria, dengue and Japanese encephalitis mosquito vectors.
685 *Ecotoxicology and Environmental Safety*, 133, 395–402. <https://doi.org/10.1016/j.ecoenv.2016.07.035>
- 686 Hamilton, J. G. C., Hall, D. R., & Kirk, W. D. J. (2005). Identification of a male-produced aggregation
687 pheromone in the western flower thrips *Frankliniella occidentalis*. *Journal of Chemical Ecology*, 31(6), 1369–
688 1379. <https://doi.org/10.1007/s10886-005-1351-z>
- 689 Hammer, D. A. T., Ryan, P. D., Hammer, Ø., & Harper, D. A. T. (2001). Past: Paleontological Statistics Software
690 Package for Education and Data Analysis. In *Palaeontologia Electronica* (Vol. 4, Issue 1). [http://palaeo-](http://palaeo-electronica.org)
691 [electronica.org](http://palaeo-electronica.org/2001_1/past/issue1_01.htm)http://palaeo-electronica.org/2001_1/past/issue1_01.htm.
- 692 Holkenbrink, C., Ding, B. J., Wang, H. L., Dam, M. I., Petkevicius, K., Kildegaard, K. R., Wenning, L., Sinkwitz,
693 C., Lorántfy, B., Koutsoumpeli, E., França, L., Pires, M., Bernardi, C., Urrutia, W., Mafra-Neto, A., Ferreira, B.
694 S., Raptopoulos, D., Konstantopoulou, M., Löfstedt, C., & Borodina, I. (2020). Production of moth sex
695 pheromones for pest control by yeast fermentation. *Metabolic Engineering*, 62, 312–321.
696 <https://doi.org/10.1016/j.ymben.2020.10.001>
- 697 Huchelmann, A., Boutry, M., & Hachez, C. (2017). Plant glandular trichomes: Natural cell factories of high
698 biotechnological interest. *Plant Physiology*, Vol. 175, Issue 1, pp. 6–22. American Society of Plant Biologists.
699 <https://doi.org/10.1104/pp.17.00727>
- 700 Ioriatti, C., & Lucchi, A. (2016). Semiochemical Strategies for Tortricid Moth Control in Apple Orchards and
701 Vineyards in Italy. *Journal of Chemical Ecology*, 42(7), 571–583. [https://doi.org/10.1007/s10886-016-0722-](https://doi.org/10.1007/s10886-016-0722-y)
702 [y](https://doi.org/10.1007/s10886-016-0722-y)
- 703 Juteršek, M., Gerasymenko, I. M., Petek, M., Haumann, E., González, S. V., Kallam, K., Gianoglio, S., Navarro-
704 Llopis, V., Fuertes, I. N., Patron, N., Orzáez, D., Gruden, K., Warzecha, H., & Baebler, Š. (2023). Identification
705 and characterisation of *Planococcus citri* *cis*- and *trans*-isoprenyl diphosphate synthase genes, supported by
706 short- and long-read transcriptome data. *BioRxiv*, 2023.06.09.544309.
707 <https://doi.org/10.1101/2023.06.09.544309>
- 708 Kallam, K., Moreno-Giménez, E., Mateos-Fernández, R., Tansley, C., Gianoglio, S., Orzaez, D., & Patron, N.
709 (2023). Tunable control of insect pheromone biosynthesis in *Nicotiana benthamiana*. *Plant Biotechnology*
710 *Journal*. <https://doi.org/10.1111/pbi.14048>
- 711 Klassen, D., Lennox, M. D., Dumont, M. J., Chouinard, G., & Tavares, J. R. (2023). Dispensers for pheromonal
712 pest control. In *Journal of Environmental Management* (Vol. 325). Academic Press.
713 <https://doi.org/10.1016/j.jenvman.2022.116590>

- 714 Kobayashi, M., & Kuzuyama, T. (2019). Structural and Mechanistic Insight into Terpene Synthases that
715 Catalyze the Irregular Non-Head-to-Tail Coupling of Prenyl Substrates. In *ChemBioChem* (Vol. 20, Issue 1, pp.
716 29–33). Wiley-VCH Verlag. <https://doi.org/10.1002/cbic.201800510>
- 717 Li, J., Mutanda, I., Wang, K., Yang, L., Wang, J., & Wang, Y. (2019). Chloroplastic metabolic engineering
718 coupled with isoprenoid pool enhancement for committed taxanes biosynthesis in *Nicotiana benthamiana*.
719 *Nature Communications*, 10(1). <https://doi.org/10.1038/s41467-019-12879-y>
- 720 Löfstedt, C., Wahlberg, N., and Millar, J.G. 'Evolutionary patterns of pheromone diversity in Lepidoptera' in
721 Pheromone Communication in Moths, J.D. Allison and R.T. Cardé, Eds., pp.43–78, University of California
722 Press, Berkeley, 2016.
- 723 Loughrin, J. H., Hamilton-Kemp, T. R., Andersen, R. A., & Hildebrand, D. F. (1991). Circadian rhythm of volatile
724 emission from flowers of *Nicotiana sylvestris* and *N. suaveolens*. *Physiologia Plantarum*, 83(3), 492–496.
725 <https://doi.org/10.1111/j.1399-3054.1991.tb00125.x>
- 726 Lucchi, A., Suma, P., Ladurner, E., Iodice, A., Savino, F., Ricciardi, R., Cosci, F., Marchesini, E., Conte, G., and
727 Benelli, G. (2019). Managing the vine mealybug, *Planococcus ficus*, through pheromone-mediated mating
728 disruption. *Environmental Science and Pollution Research*, 10708-10718, 26(11).
729 <https://doi.org/10.1007/s11356-019-04530-6>
- 730 Mani, V., Park, S., Kim, J. A., Lee, S. I., & Lee, K. (2021). Metabolic perturbation and synthetic biology
731 strategies for plant terpenoid production—An updated overview. In *Plants* (Vol. 10, Issue 10). MDPI.
732 <https://doi.org/10.3390/plants10102179>
- 733 Mateos Fernández, R., Petek, M., Gerasymenko, I., Juteršek, M., Baebler, Š., Kallam, K., Moreno Giménez, E.,
734 Gondolf, J., Nordmann, A., Gruden, K., Orzaez, D., & Patron, N. J. (2022). Insect pest management in the age
735 of synthetic biology. *Plant Biotechnology Journal*, 20(1), 25–36. <https://doi.org/10.1111/pbi.13685>
- 736 Mateos-Fernández, R., Moreno-Giménez, E., Gianoglio, S., Quijano-Rubio, A., Gavaldá-García, J., Estellés, L.,
737 Rubert, A., Rambla, J. L., Vazquez-Vilar, M., Huet, E., Fernández-Del-Carmen, A., Espinosa-Ruiz, A., Juteršek,
738 M., Vacas, S., Navarro, I., Navarro-Llopis, V., Primo, J., & Orzáez, D. (2021). Production of Volatile Moth Sex
739 Pheromones in Transgenic *Nicotiana benthamiana* Plants. *BioDesign Research*, 2021.
740 <https://doi.org/10.34133/2021/9891082>
- 741 Miller, J. R., & Gut, L. J. (2015). Mating disruption for the 21st century: Matching technology with mechanism.
742 In *Environmental Entomology* (Vol. 44, Issue 3, pp. 427–453). Entomological Society of America.
743 <https://doi.org/10.1093/ee/nvv052>
- 744 Minteguiga, M., Catalán, C. A. N., & Dellacassa, E. (2023). Irregular Monoterpenes in Essential Oils with
745 Special Emphasis on ortho-Menthane Derivatives. In *ACS Symposium Series* (Vol. 1433, pp. 361–383).
746 American Chemical Society. <https://doi.org/10.1021/bk-2022-1433.ch009>
- 747 Möhring, N., Ingold, K., Kudsk, P., Martin-Laurent, F., Niggli, U., Siegrist, M., Studer, B., Walter, A., & Finger,
748 R. (2020). Pathways for advancing pesticide policies. In *Nature Food* (Vol. 1, Issue 9, pp. 535–540). Springer
749 Nature. <https://doi.org/10.1038/s43016-020-00141-4>
- 750 Molina-Hidalgo, F. J., Vazquez-Vilar, M., D'Andrea, L., Demurtas, O. C., Fraser, P., Giuliano, G., Bock, R.,
751 Orzáez, D., & Goossens, A. (2021). Engineering Metabolism in *Nicotiana* Species: A Promising Future. In
752 *Trends in Biotechnology* (Vol. 39, Issue 9, pp. 901–913). Elsevier Ltd.
753 <https://doi.org/10.1016/j.tibtech.2020.11.012>
- 754 Nešňorová, P., Šebek, P., Macek, T., & Svatoš, A. (2004). First semi-synthetic preparation of sex pheromones.
755 *Green Chemistry*, 6(7), 305–307. <https://doi.org/10.1039/b406814a>

- 756 Pepper, H. P., Tulip, S. J., Nakano, Y., & George, J. H. (2014). Biomimetic total synthesis of (±)-
757 doitunggarcinone A and (+)-garcibracteatone. *The Journal of Organic Chemistry*, 79(6), 2564–2573.
758 <https://doi.org/10.1021/jo500027k>
- 759 Petkevicius, K., Löfstedt, C., & Borodina, I. (2020). Insect sex pheromone production in yeasts and plants. In
760 *Current Opinion in Biotechnology* (Vol. 65, pp. 259–267). Elsevier Ltd.
761 <https://doi.org/10.1016/j.copbio.2020.07.011>
- 762 Poulter, C. D., Marsh, L. L., Hughes, J. M., Argyle, J. C., Satterwhite, D. M., Goodfellow, R. J., & Moesinger, S.
763 G. (1977). Model Studies of the Biosynthesis of Non-Head-to-Tail Terpenes. Rearrangements of the
764 Chrysanthemyl System. *Journal of the American Chemical Society*, 99(11), 3816–3823.
765 <https://doi.org/10.1021/ja00453a050>
- 766 Rivera, S. B., Swedlund, B. D., King, G. J., Bell, R. N., Hussey, C. E., Shattuck-Eidens, D. M., Wrobel, W. M.,
767 Peiser, G. D., & Poulter, C. D. (2001). Chrysanthemyl diphosphate synthase: Isolation of the gene and
768 characterization of the recombinant non-head-to-tail monoterpene synthase from *Chrysanthemum*
769 *cinerariaefolium*. *Proceedings of the National Academy of Sciences of the United States of America*, 98(8),
770 4373–4378. <https://doi.org/10.1073/pnas.071543598>
- 771 Rizvi, S. A. H., George, J., Reddy, G. V. P., Zeng, X., & Guerrero, A. (2021). Latest developments in insect sex
772 pheromone research and its application in agricultural pest management. In *Insects* (Vol. 12, Issue 6). MDPI
773 AG. <https://doi.org/10.3390/insects12060484>
- 774 Sarker, L. S., & Mahmoud, S. S. (2015). Cloning and functional characterization of two monoterpene
775 acetyltransferases from glandular trichomes of *L. x intermedia*. *Planta*, 242(3), 709–719.
776 <https://doi.org/10.1007/s00425-015-2325-1>
- 777 Sarrion-Perdigones, A., Falconi, E. E., Zandalinas, S. I., Juárez, P., Fernández-del-Carmen, A., Granell, A., &
778 Orzaez, D. (2011). GoldenBraid: An iterative cloning system for standardized assembly of reusable genetic
779 modules. *PLoS ONE*, 6(7). <https://doi.org/10.1371/journal.pone.0021622>
- 780 Schmidt, F.J., Zimmermann, M.M., Wiedmann, D.R., Lichtenauer, S., Grundmann, L., Muth, J., Twyman, R.M.,
781 Prüfer, D., and Noll, G.A. (2020). The Major Floral Promoter NtFT5 in Tobacco (*Nicotiana tabacum*) Is a
782 Promising Target for Crop Improvement. *Front. Plant Sci.*, Volume 10 - 2019 |
783 <https://doi.org/10.3389/fpls.2019.01666>
- 784 Tabata, J. (2022). Genetic Basis Underlying Structural Shift of Monoterpenoid Pheromones in Mealybugs.
785 *Journal of Chemical Ecology*, 48(5–6), 546–553. <https://doi.org/10.1007/s10886-021-01339-x>
- 786 Tissier, A., Morgan, J. A., & Dudareva, N. (2017). Plant Volatiles: Going ‘In’ but not ‘Out’ of Trichome Cavities.
787 In *Trends in Plant Science* (Vol. 22, Issue 11, pp. 930–938). Elsevier Ltd.
788 <https://doi.org/10.1016/j.tplants.2017.09.001>
- 789 Wang, H., Jiang, G., Liang, N., Dong, T., Shan, M., Yao, M., Wang, Y., Xiao, W., & Yuan, Y. (2022). Systematic
790 Engineering to Enhance 8-Hydroxygeraniol Production in Yeast. *Journal of Agricultural and Food Chemistry*.
791 <https://doi.org/10.1021/acs.jafc.2c09028>
- 792 Wang, Q., Quan, S., & Xiao, H. (2019). Towards efficient terpenoid biosynthesis: manipulating IPP and
793 DMAPP supply. In *Bioresources and Bioprocessing* (Vol. 6, Issue 1). Springer Science and Business Media
794 Deutschland GmbH. <https://doi.org/10.1186/s40643-019-0242-z>
- 795 Wang, Y., Wen, J., Liu, L., Chen, J., Wang, C., Li, Z., Wang, G., Pichersky, E., & Xu, H. (2022). Engineering of
796 tomato type VI glandular trichomes for trans-chrysanthemoid acid biosynthesis, the acid moiety of natural
797 pyrethrin insecticides. *Metabolic Engineering*, 72, 188–199. <https://doi.org/10.1016/j.ymben.2022.03.007>

- 798 Wu, S., Schalk, M., Clark, A., Miles, R. B., Coates, R., & Chappell, J. (2006). Redirection of cytosolic or plastidic
799 isoprenoid precursors elevates terpene production in plants. *Nature Biotechnology*, 24(11), 1441–1447.
800 <https://doi.org/10.1038/nbt1251>
- 801 Xia, Y. H., Ding, B. J., Wang, H. L., Hofvander, P., Jarl-Sunesson, C., & Löfstedt, C. (2020). Production of moth
802 sex pheromone precursors in *Nicotiana* spp.: a worthwhile new approach to pest control. *Journal of Pest*
803 *Science*, 93(4), 1333–1346. <https://doi.org/10.1007/s10340-020-01250-6>
- 804 Xie, S. S., Zhu, L., Qiu, X. Y., Zhu, C. S., & Zhu, L. Y. (2019). Advances in the metabolic engineering of *Escherichia*
805 *coli* for the manufacture of monoterpenes. *Catalysts*, 9(5). <https://doi.org/10.3390/catal9050433>
- 806 Xu, H., Lybrand, D., Bennewitz, S., Tissier, A., Last, R. L., & Pichersky, E. (2018). Production of *trans*-
807 chrysanthemoid acid, the monoterpene acid moiety of natural pyrethrin insecticides, in tomato fruit.
808 *Metabolic Engineering*, 47, 271–278. <https://doi.org/10.1016/j.ymben.2018.04.004>
- 809 Xu, H., Moghe, G. D., Wiegert-Rininger, K., Schillmiller, A. L., Barry, C. S., Last, R. L., & Pichersky, E. (2018).
810 Coexpression analysis identifies two oxidoreductases involved in the biosynthesis of the monoterpene acid
811 moiety of natural pyrethrin insecticides in *Tanacetum cinerariifolium*. *Plant Physiology*, 176(1), 524–537.
812 <https://doi.org/10.1104/pp.17.01330>
- 813 Yang, T., Gao, L., Hu, H., Stoop, G., Wang, C., & Jongsma, M. A. (2014). Chrysanthemyl diphosphate
814 synthase operates *in planta* as a bifunctional enzyme with chrysanthemol synthase activity. *Journal of*
815 *Biological Chemistry*, 289(52), 36325–36335. <https://doi.org/10.1074/jbc.M114.623348>
- 816 Yin, J. L., Wong, W. S., Jang, I. C., & Chua, N. H. (2017). Co-expression of peppermint geranyl diphosphate
817 synthase small subunit enhances monoterpene production in transgenic tobacco plants. *New Phytologist*,
818 213(3), 1133–1144. <https://doi.org/10.1111/nph.14280>
- 819 Zielińska-Błajet, M., & Feder-Kubis, J. (2020). Monoterpenes and their derivatives—recent development in
820 biological and medical applications. In *International Journal of Molecular Sciences* (Vol. 21, Issue 19, pp. 1–
821 38). MDPI AG. <https://doi.org/10.3390/ijms21197078>
- 822 Zou, Y., & Millar, J. G. (2015). Chemistry of the pheromones of mealybug and scale insects. *Natural Product*
823 *Reports*, 32(7), 1067–1113. <https://doi.org/10.1039/c4np00143e>
- 824
- 825
- 826
- 827
- 828
- 829
- 830
- 831
- 832
- 833
- 834

Plant	µg lavandulol g⁻¹ FW	µg chrysanthemol g⁻¹ FW
Nb LPPS 11_2_4_7	30.1	-
Nb LPPS 11_2_4_8	29.7	-
Nb LPPS 11_2_4_9	44.6	-
Mean ± sd	34.8 ± 8.5	-
Nb CPPS 5_4_1_7	-	0.61
Nb CPPS 5_4_1_8	-	0.49
Nb CPPS 5_4_1_9	-	0.61
Mean ± sd	-	0.60 ± 0.07
Nt LPPS_1_3_1_3	29.68	-
Nt LPPS_1_3_1_4	21.96	-
Nt LPPS_1_3_1_5	16.02	-
Mean ± sd	22.55 ± 6.85	-
Nt CPPS_1_3_2_2	-	0.43
Nt CPPS_1_3_2_3	-	0.68
Nt CPPS_1_3_2_4	-	0.76
Mean ± sd	-	0.6 ± 0.2

835

836 **Table 1.** Quantity (µg) of lavandulol and chrysanthemol obtained from young whole T₃ *NbLPPS* and *NbCPPS*
837 plants and from leaves of young T₃ *NtLPPS* and *NtCPPS* plants by solvent extraction and GC/MS/MS
838 quantification.

839

840

Plant	Material	ng lavandulol g ⁻¹ FW day ⁻¹	ng chrysanthemol g ⁻¹ FW day ⁻¹
Nb LPPS 11_2_4_7	Full plant (young)	218.42	-
Nb LPPS 11_2_4_8	Full plant (young)	96.33	-
Nb LPPS 11_2_4_9	Full plant (young)	159.91	-
Mean ± sd	Full plant (young)	158.22 ± 61.06	-
Nb CPPS 5_4_1_7	Full plant (young)	-	62.95
Nb CPPS 5_4_1_8	Full plant (young)	-	24.32
Nb CPPS 5_4_1_9	Full plant (young)	-	44.98
Mean ± sd	Full plant (young)	-	44.08 ± 19.33
Nt LPPS_1_3_1_3	Young leaves	48.61	-
Nt LPPS_1_3_1_4	Young leaves	54.59	-
Nt LPPS_1_3_1_5	Young leaves	58.48	-
Mean ± sd	Young leaves	53.89 ± 4.97	-
Nt LPPS_1_3_1_3	Flowers	168.21	-
Nt LPPS_1_3_1_4	Flowers	348.7	-
Nt LPPS_1_3_1_5	Flowers	392.11	-
Mean ± sd	Flowers	303.01 ± 118.74	-
Nt CPPS_1_3_2_2	Young leaves	-	19.04
Nt CPPS_1_3_2_3	Young leaves	-	21.72
Nt CPPS_1_3_2_4	Young leaves	-	13.54
Mean ± sd	Young leaves	-	18.1 ± 4.17
Nt CPPS_1_3_2_2	Flowers	-	45.49
Nt CPPS_1_3_2_3	Flowers	-	36.92
Nt CPPS_1_3_2_4	Flowers	-	14.08
Mean ± sd	Flowers	-	32.16 ± 16.24

841

842 **Table 2.** Quantity (ng) of lavandulol and chrysanthemol released by whole T₃ *NbLPPS* and *NbCPPS*
 843 young individuals, and by T₃ *NtLPPS* and *NtCPPS* young leaves and flowers, measured by volatile
 844 collection and GC/MS/MS quantification.

845

Plant	µg lavandulol g ⁻¹ FW	µg lavandulyl acetate g ⁻¹ FW
Nt LPPS-AAT4_4_4	16.37	0.49
Nt LPPS-AAT4_4_5	17.85	0.70
Nt LPPS-AAT4_4_6	16.85	0.56
Mean ± sd	17.02 ± 0.75	0.58 ± 0.11
Nt LPPS-AAT4_8_1	10.55	0.85
Nt LPPS-AAT4_8_4	15.88	0.64
Nt LPPS-AAT4_8_6	6.49	0.46
Mean ± sd	10.97 ± 4.71	0.65 ± 0.20

846

847 **Table 3.** Quantity (µg) of lavandulol and lavandulyl acetate obtained from young leaves of T₁ *NtLPPS*-
 848 *AAT4* plants by solvent extraction and GC/MS/MS quantification.

849

Plant	Material	ng lavandulol g ⁻¹ FW day ⁻¹	ng lavandulyl acetate g ⁻¹ FW day ⁻¹
Nt LPPS-AAT4_4_4	Leaves	62.99	107.85
Nt LPPS-AAT4_4_5	Leaves	115.08	388.03
Nt LPPS-AAT4_4_6	Leaves	111.61	337.06
Mean ± sd	Leaves	96.56 ± 29.13	277 ± 149.24
Nt LPPS-AAT4_8_1	Leaves	85.93	857.68
Nt LPPS-AAT4_8_4	Leaves	93.49	555.90
Nt LPPS-AAT4_8_6	Leaves	37.93	466.92
Mean ± sd	Leaves	72.45 ± 30.13	626.84 ± 204.81
Nt LPPS-AAT4_8_1	Flowers	166.10	167.58
Nt LPPS-AAT4_8_3	Flowers	191.31	411.09
Nt LPPS-AAT4_8_6	Flowers	118.78	180.00
Mean ± sd	Flowers	158.73 ± 36.82	252.89 ± 137.14

850

851

852

Table 4. Quantity (ng) of lavandulol and lavandulyl acetate released from organs (leaves and flowers) of T₁ *NtLPPS-AAT4* plants, obtained by volatile collection and GC/MS/MS quantification.

853

854 Figure legends

855 **Figure 1. Production of the volatile monoterpenoids lavandulol and chrysanthemol in transient expression**
856 **in *N. benthamiana*.** (A) Biosynthetic metabolic pathway of the irregular monoterpenoids lavandulyl
857 pyrophosphate and chrysanthemyl pyrophosphate via the non-head-to-tail condensation of two DMAPP by
858 the LPPS or CPPS enzyme. Production of the alcohols might be due to host endogenous phosphatases or to
859 a bifunctional activity of these irregular IDSs. (B) The T-DNA construct used for transient expression of *LiLPPS*
860 controlled by the CaMV35S promoter and Nos terminator, and the GC-MS profile of *N. benthamiana* leaf
861 tissue 5 dpi. (C) The T-DNA construct used for transient expression of *TcCPPS* controlled by the CaMV35S
862 promoter and Nos terminator, and the GC-MS profile of *N. benthamiana* leaf tissue 5 dpi. (D) The GC-MS
863 profile of *N. benthamiana* leaf tissue 5 dpi in negative control plants infiltrated only with the P19 silencing
864 suppressor. (E) Lavandulol, chrysanthemol, and chrysanthemol-derived compounds measured by GC-MS in
865 agroinfiltrated *N. benthamiana* leaves.

866 **Figure 2. Physiological effect of irregular monoterpene production in T₃ *N. benthamiana* and tobacco**
867 **plants.** Comparison of flowering time (A), plant size at 100 days (B) and total biomass reached at 100 days
868 (C) in *NbLPPS*, *NbCPPS* and WT plants. In panel (A), time measured as days from transfer to soil to anthesis
869 of the first flower. (D) Phenotype of *NbLPPS* and *NbCPPS* plants compared to WT at 24 and 48 days in soil.
870 Comparison of flowering time (E), plant size at flowering (F) and total foliar biomass accumulated at harvest
871 time (140 days) (G) in *NtLPPS*, *NtCPPS* and WT plants. In panel (E), time measured as days from transfer to
872 soil to formation of the floral meristem. (H) Phenotype of *NtLPPS* and *NtCPPS* plants compared to WT at 35
873 and 75 days in soil. Values are the mean and standard deviation of at least 3 independent plants of each line.
874 Error bars with the same letter are not significantly different (one-way ANOVA with post-hoc Tukey HSD at
875 the 5% level of significance).

876 **Figure 3. Comparison of lavandulol and chrysanthemol production in leaves at different developmental**
877 **stages of T₃ *N. benthamiana* and tobacco plants.** (A) Lavandulol production in *NbLPPS_11_2_4* and
878 *NbLPPS_5_2_2* lines. (B) Chrysanthemol production in *NbCPPS_5_4_1* line. (C) Lavandulol production in
879 *NtLPPS_1_3_1* and *NtLPPS_3_1_3* lines. (D) Chrysanthemol production in *NtCPPS_1_3_2* line. In panels (A)
880 and (B) values are reported for two plant growth stages (pre-flowering and post-flowering) and for three leaf
881 developmental stages (Y=young, A=adult, S=senescent). In panels (C) and (D) values are reported for three
882 types of leaves (Y=young, A=adult, S=senescent). Production values represent the mean and standard
883 deviation of n = 3 biological replicates (independent leaves). All data for this figure, together with statistical
884 analyses (two-way ANOVA) are reported in Supplementary Data File S1.

885 **Figure 4. Production of lavandulol and chrysanthemol in T₃ *N. benthamiana* and tobacco plants in different**
886 **tissue types.** (A) Lavandulol production in vegetative and reproductive tissue in line *NbLPPS_11_2_4*,
887 measured in homogenized and intact organs. (B) Chrysanthemol production in reproductive and vegetative
888 tissue in line *NbCPPS_5_4_1*, measured in homogenized and intact organs. (C) Lavandulol production in
889 vegetative and reproductive tissues in line *NtLPPS_1_3_1*, measured in homogenized leaves and flowers. (D)
890 Chrysanthemol production in vegetative and reproductive tissue in line *NtCPPS_1_3_2*, measured in
891 homogenized leaves and flowers. In all panels, leaf tissues are denoted as “L” and flower tissues as “F”. In
892 panels (C) and (D) values are reported for three types of leaves (Y=young, A=adult, S=senescent). Values
893 represent the mean and SD of n=3 biological replicates (independent organs). Comparisons (Student’s *t* and
894 Mann-Whitney’s test for *N. benthamiana* and one-way ANOVA with HSD Tukey’s posthoc test, $p < 0.05$) were
895 carried out between samples undergoing the same treatment (homogenized or intact). Letters identify
896 significance groups.

897 **Figure 5. Esterification of lavandulol to lavandulyl acetate.** (A) Constructs carrying the *LiAAT4* transgene
898 controlled by the CAMV35s promoter and NOS terminator and the silencing suppressor P19, and the design
899 of the agroinfiltration assay. (B) Levels of lavandulyl acetate obtained by infiltrating *LiAAT4* in *NbLPPS* T₃

900 plants (*NbLPPS_11_2_4* background); for each individual, '-' indicates infiltration with P19 alone, while '+'
901 indicates infiltration with *LiAAT4* and P19. Positive controls are represented by WT leaves infiltrated with
902 *LiLPPS* alone (LPPS C+) and with *LiLPPS* and *LiAAT4* (LPPS AAT4 C+), always combined with P19. The negative
903 control is represented by WT plants infiltrated only with P19 (C-). **(C)** Production of lavandulol and lavandulyl
904 acetate in the T₁ progeny of *NtLPPS_AAT4_8*; values are reported for three types of leaves (Y=young,
905 A=adult, S=senescent). **(D)** Production of lavandulol and lavandulyl acetate in reproductive (indicated as F)
906 and vegetative (indicated as L) tissues (ground samples) of T₁ *NtLPPS_AAT4_8* plants. Three types of leaves
907 are analyzed (Y=young, A=adult, S=senescent). Comparison of flowering time **(E)**, plant size at flowering **(F)**
908 and total foliar biomass accumulated at harvest time (140 days) **(G)** in *NtLPPS_AAT4* and WT plants. In panel
909 (E), time measured as days from transfer to soil to formation of the floral meristem in T₁ *NtLPPS_AAT4* and
910 WT plants. **(H)** Phenotype of T₁ *NtLPPS_AAT4_8* plants compared to the WT at 35 and 75 days in soil. In
911 panels (B), (C) and (D) values are the mean and standard deviation of 3 independent samples. In panels (E),
912 (F) and (G), values are the mean and standard deviation of at least 3 independent plants of each line. *P*-
913 values were calculated using Student's *t*-test; **P* ≤ 0.05, ***P* ≤ 0.01. The figure includes images from
914 Biorender (biorender.com).

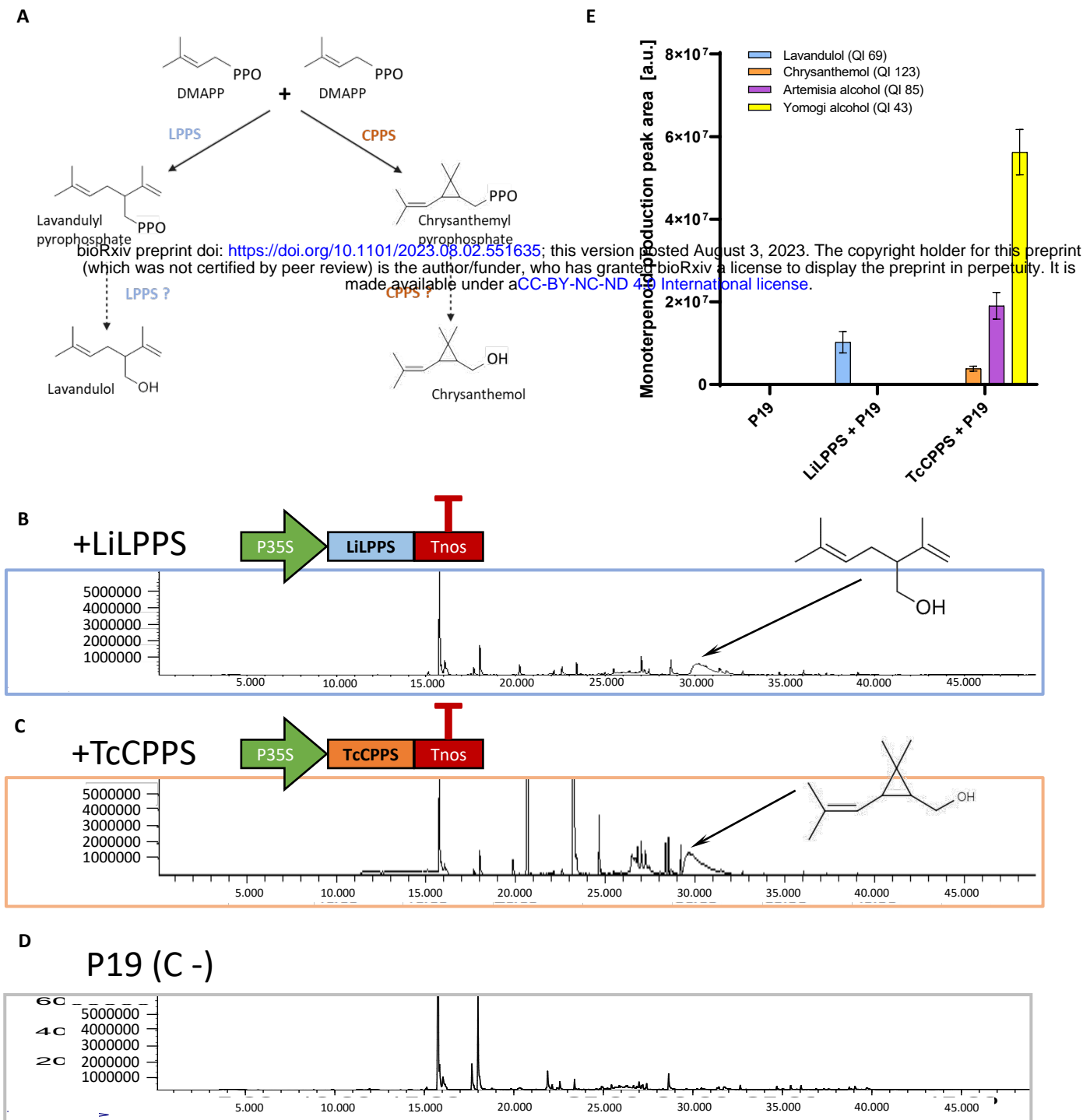
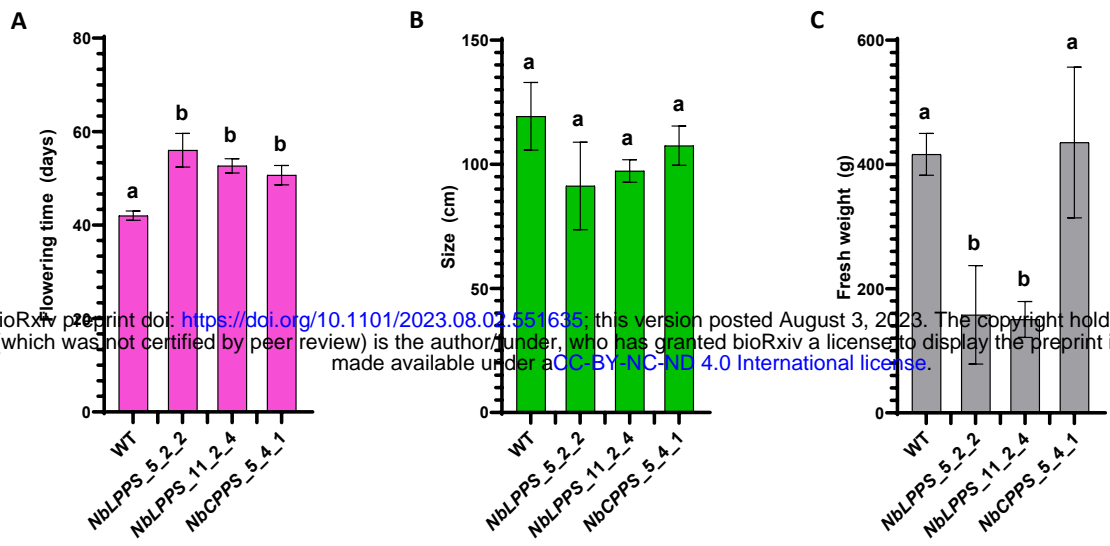


Figure 1. Production of the volatile monoterpenoids lavandulol and chrysanthemol in transient expression in *N. benthamiana*. (A) Biosynthetic metabolic pathway of the irregular monoterpenoids lavandulyl pyrophosphate and chrysanthemyl pyrophosphate via the non-head-to-tail condensation of two DMAPP by the LPPS or CPPS enzyme. Production of the alcohols might be due to host endogenous phosphatases or to a bifunctional activity of these irregular IDs. (B) The T-DNA construct used for transient expression of *LiLPPS* controlled by the CaMV35S promoter and Nos terminator, and the GC-MS profile of *N. benthamiana* leaf tissue 5 dpi. (C) The T-DNA construct used for transient expression of *TcCPPS* controlled by the CaMV35S promoter and Nos terminator, and the GC-MS profile of *N. benthamiana* leaf tissue 5 dpi. (D) The GC-MS profile of *N. benthamiana* leaf tissue 5 dpi in negative control plants infiltrated only with the P19 silencing suppressor. (E) Lavandulol, chrysanthemol, and chrysanthemol-derived compounds measured by GC-MS in agroinfiltrated *N. benthamiana* leaves.



bioRxiv preprint doi: <https://doi.org/10.1101/2023.08.03.551635>; this version posted August 3, 2023. The copyright holder for this preprint (which was not certified by peer review) is the author/funder, who has granted bioRxiv a license to display the preprint in perpetuity. It is made available under aCC-BY-NC-ND 4.0 International license.

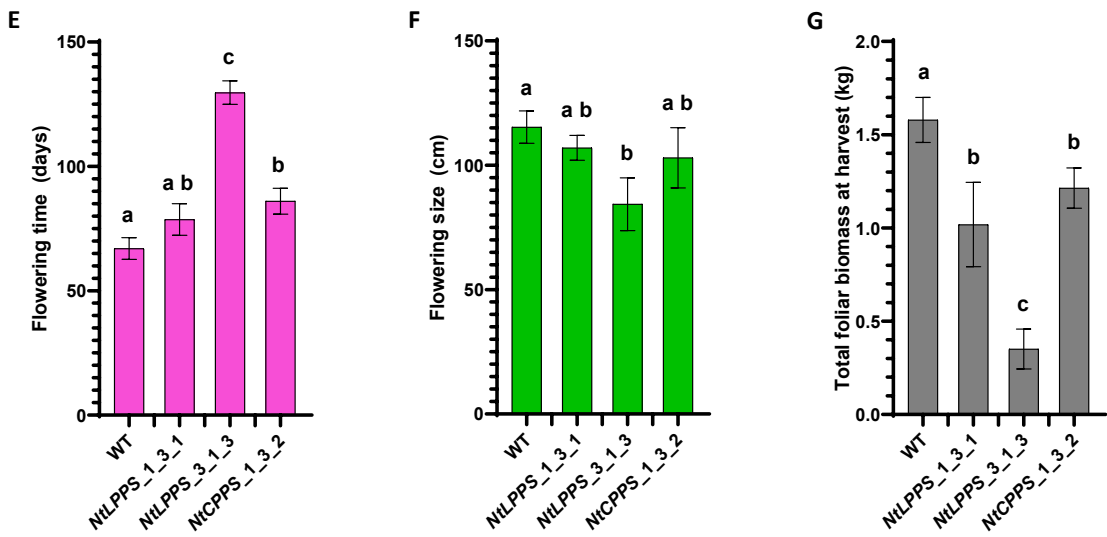


Figure 2. Physiological effect of irregular monoterpene production in T_3 *N. benthamiana* and tobacco plants. Comparison of flowering time (**A**), plant size at 100 days (**B**) and total biomass reached at 100 days (**C**) in *NbLPPS*, *NbCPPS* and WT plants. In panel (A), time measured as days from transfer to soil to anthesis of the first flower. (**D**) Phenotype of *NbLPPS* and *NbCPPS* plants compared to WT at 24 and 48 days in soil. Comparison of flowering time (**E**), plant size at flowering (**F**) and total foliar biomass accumulated at harvest time (140 days) (**G**) in *NtLPPS*, *NtCPPS* and WT plants. In panel (**E**), time measured as days from transfer to soil to formation of the floral meristem. (**H**) Phenotype of *NtLPPS* and *NtCPPS* plants compared to WT at 35 and 75 days in soil. Values are the mean and standard deviation of at least 3 independent plants of each line. Error bars with the same letter are not significantly different (one-way ANOVA with post-hoc Tukey HSD at the 5% level of significance).

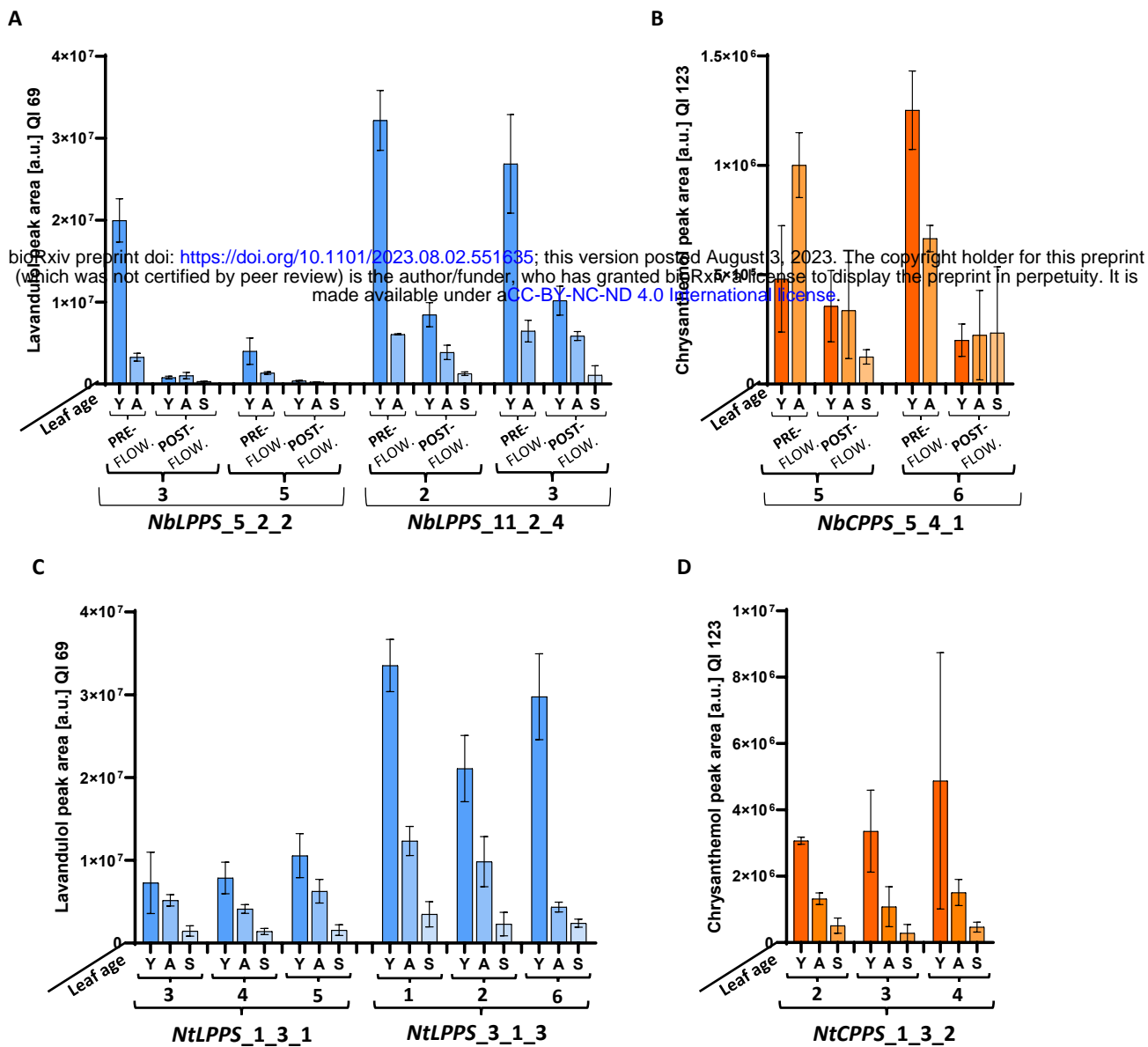


Figure 3. Comparison of lavandulol and chrysanthemol production in leaves at different developmental stages of T3 *N. benthamiana* and tobacco plants. (A) Lavandulol production in *NbLPPS_11_2_4* and *NbLPPS_5_2_2* lines. **(B)** Chrysanthemol production in *NbCPS_5_4_1* line. **(C)** Lavandulol production in *NtLPPS_1_3_1* and *NtLPPS_3_1_3* lines. **(D)** Chrysanthemol production in *NtCPS_1_3_2* line. In panels (A) and (B) values are reported for two plant growth stages (pre-flowering and post-flowering) and for three leaf developmental stages (Y=young, A=adult, S=senescent). In panels (C) and (D) values are reported for three types of leaves (Y=young, A=adult, S=senescent). Production values represent the mean and standard deviation of $n = 3$ biological replicates (independent leaves). All data for this figure, together with statistical analyses (two-way ANOVA), are reported in Supplementary Data File S1.

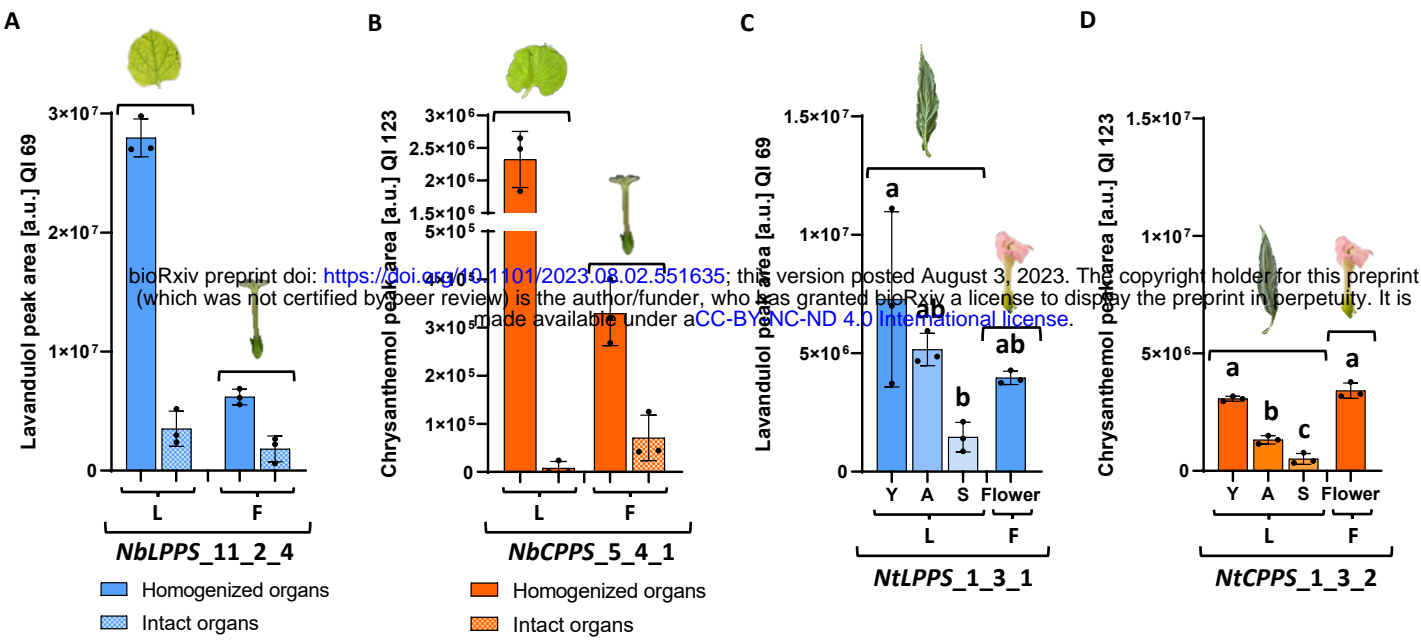
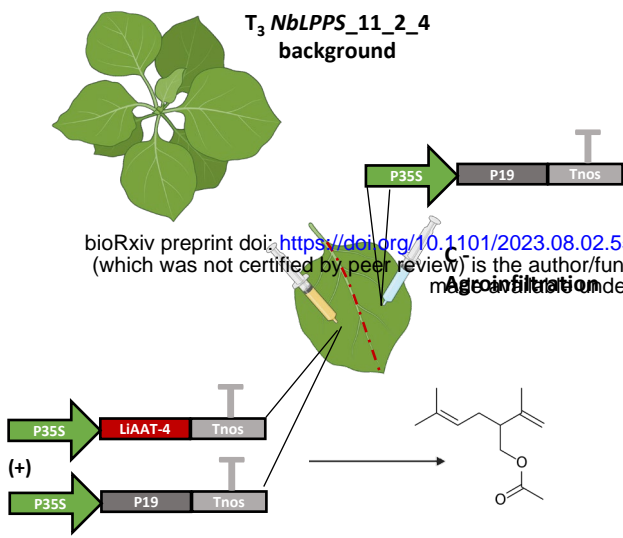
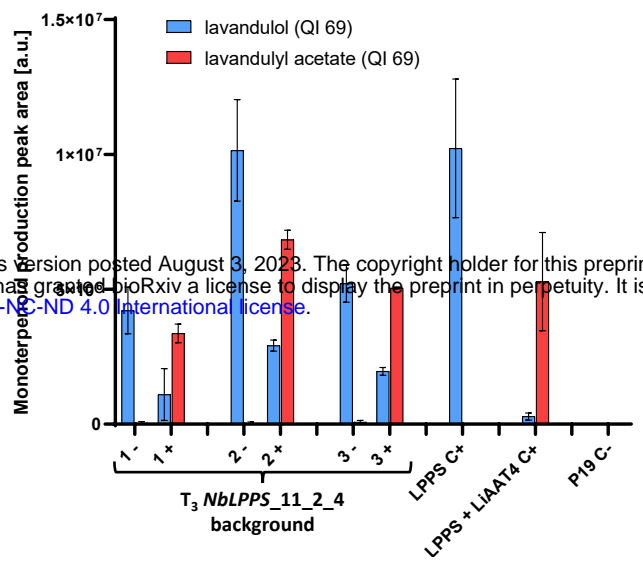


Figure 4. Production of lavandulol and chrysanthemol in T₃ *N. benthamiana* and tobacco plants in different tissue types. (A) Lavandulol production in vegetative and reproductive tissue in line *NbLPPS_11_2_4*, measured in homogenized and intact organs. **(B)** Chrysanthemol production in reproductive and vegetative tissue in line *NbCPS_5_4_1*, measured in homogenized and intact organs. **(C)** Lavandulol production in vegetative and reproductive tissues in line *NtLPPS_1_3_1*, measured in homogenized leaves and flowers. **(D)** Chrysanthemol production in vegetative and reproductive tissue in line *NtCPS_1_3_2*, measured in homogenized leaves and flowers. In all panels, leaf tissues are denoted as “L” and flower tissues as “F”. In panels (C) and (D) values are reported for three types of leaves (Y=young, A=adult, S=senescent). Values represent the mean and SD of n=3 biological replicates (independent organs). Comparisons (Student’s *t* and Mann-Whitney’s test for *N. benthamiana* and one-way ANOVA with HSD Tukey’s posthoc test, *p*<0.05) were carried out between samples undergoing the same treatment (homogenized or intact). Letters identify significance groups.

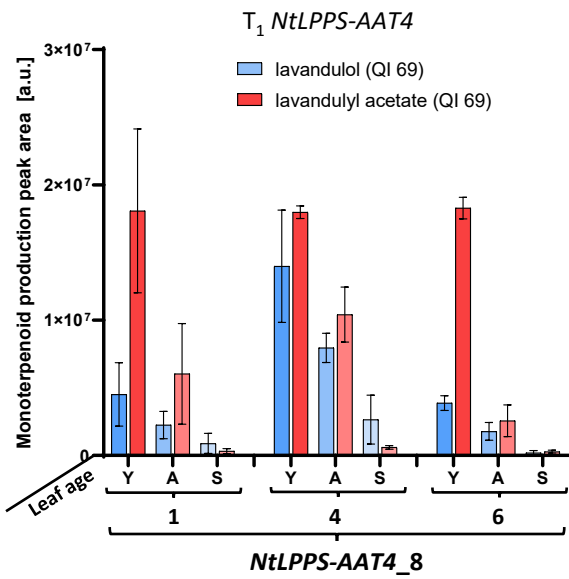
A



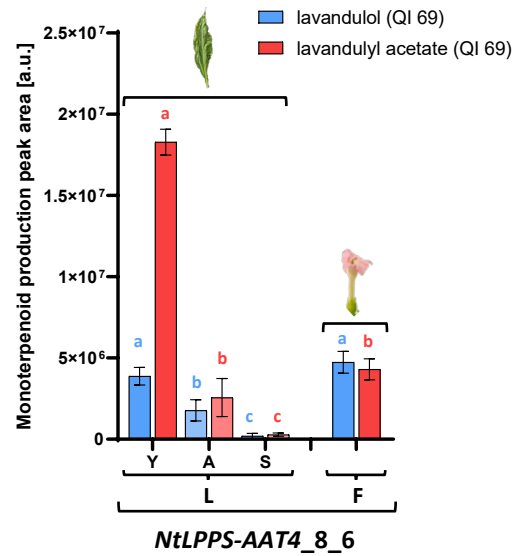
B



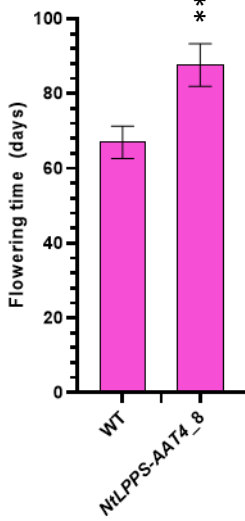
C



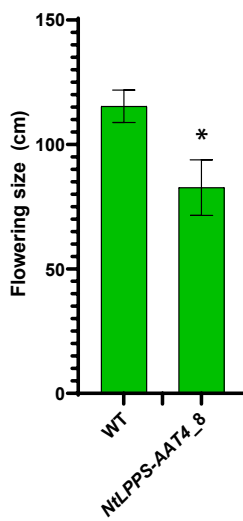
D



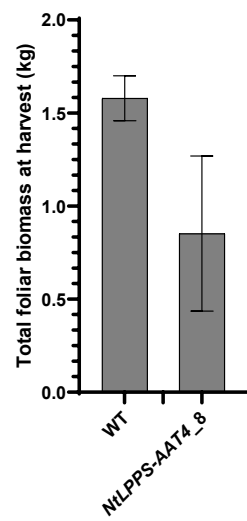
E



F



G



H

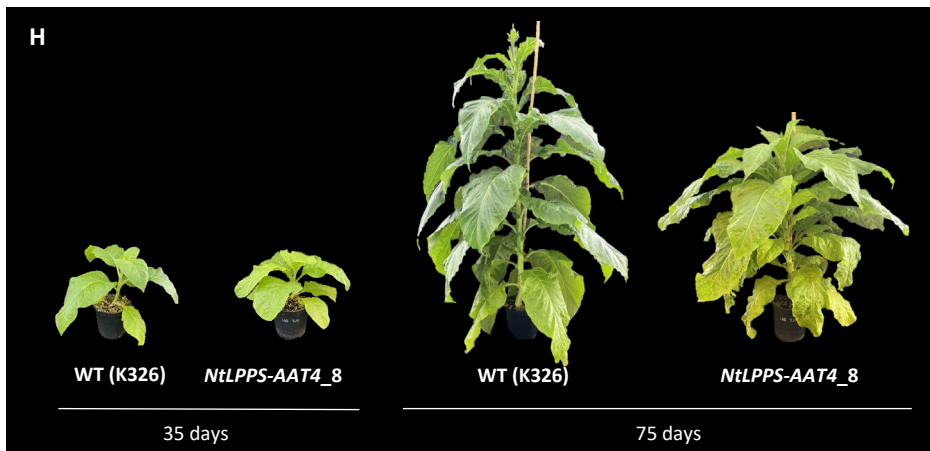


Figure 5. Esterification of lavandulol to lavandulyl acetate. (A) Constructs carrying the *LiAAT4* transgene controlled by the CAMV35s promoter and NOS terminator and the silencing suppressor P19, and the design of the agroinfiltration assay. **(B)** Levels of lavandulyl acetate obtained by infiltrating *LiAAT4* in *NbLPPS* T₃ plants (*NbLPPS_11_2_4* background); for each individual, '-' indicates infiltration with P19 alone, while '+' indicates infiltration with *LiAAT4* and P19. Positive controls are represented by WT leaves infiltrated with *LiLPPS* alone (*LPPS C+*) and with *LiLPPS* and *LiAAT4* (*LPPS_AAT4 C+*), always combined with P19. The negative control is represented by WT plants infiltrated only with P19 (*C-*). **(C)** Production of YAVG, ND, Uol and lavandulyl acetate in the T₁ progeny of *NtLPPS_AAT4_8*; values are reported for three types of leaves (Y=young, A=adult, S=senescent). **(D)** Production of lavandulol and lavandulyl acetate in reproductive (indicated as F) and vegetative (indicated as L) tissues (ground samples) of T₁ *NtLPPS_AAT4_8* plants. Three types of leaves are analyzed (Y=young, A=adult, S=senescent). Comparison of flowering time **(E)**, plant size at flowering **(F)** and total foliar biomass accumulated at harvest time (140 days) **(G)** in *NtLPPS_AAT4* and WT plants. In panel (E), time measured as days from transfer to soil to formation of the floral meristem in T₁ *NtLPPS_AAT4* and WT plants. **(H)** Phenotype of T₁ *NtLPPS_AAT4_8* plants compared to the WT at 35 and 75 days in soil. In panels (B), (C) and (D) values are the mean and standard deviation of 3 independent samples. In panels (E), (F) and (G), values are the mean and standard deviation of at least 3 independent plants of each line. *P*-values were calculated using Student's *t*-test; **P* ≤ 0.05, ***P* ≤ 0.01. The figure includes images from Biorender (biorender.com).